DOT/FAA/TC-14/19

Federal Aviation Administration
William J. Hughes Technical Center
Aviation Research Division
Atlantic City International Airport
New Jersey 08405

Simulating Laminated Composite Materials Using LS-DYNA Material Model MAT54: Single-Element Investigation

February 2015

Final Report

U.S. Department of Transportation
Federal Aviation Administration

NOTICE

Technical Report Documentation Page

1. Report No.	2. Government Accession No.	3. Recipient's Catalog No.
DOT/FAA/TC-14/19		

4. Title and Subtitle	5. Report Date
SIMULATING LAMINATED COMPOSITE MATERIALS USING LS-DYNA MATERIAL MODEL MAT54: SINGLE-ELEMENT INVESTIGATION	February 2015
	6. Performing Organization Code

7. Author(s)	8. Performing Organization Report No.
Bonnie Wade, Paolo Feraboli, Morgan Osborne, and Mostafa Rassaian	

9. Performing Organization Name and Address	10. Work Unit No. (TRAIS)
Automobili Lamborghini Advanced Composite Structures Laboratory William E. Boeing Department of Aeronautics and Astronautics University of Washington Seattle, WA 98195-2400	11. Contract or Grant No.

12. Sponsoring Agency Name and Address	13. Type of Report and Period Covered
U.S. Department of Transportation Federal Aviation Administration William J. Hughes Technical Center Aviation Research Division Aircraft Systems & Structures Branch Atlantic City International Airport, NJ 08405	14. Sponsoring Agency Code AIR-100

15. Supplementary Notes

The Federal Aviation Administration William J. Hughes Technical Center Aviation Research Division Technical Monitor was Allan Abramowitz.

16. Abstract

The basic behavior of a progressive failure model that simulates laminated composite materials was investigated. The LS-DYNA material model MAT54, Enhanced Composite Damage, is often used to simulate damage progression in dynamic simulations because it requires a reduced number of experimental input parameters compared to damage mechanics-based material models. Some shortcomings in the material model arise as a consequence of oversimplification of the complex physical mechanics that occur during failure of composite material systems. To accurately use this material model, these shortcomings must be identified, as well as the solutions to properly address them. Furthermore, MAT54 has been commonly used to simulate fabric composite materials in crash and impact simulations, although it is designed specifically to simulate orthotropic materials, such as unidirectional (UD) tape composite laminates. To evaluate the fundamental elastic, failure initiation, and post-failure behaviors of MAT54, as well as the suitability of MAT54 to model fabric composite material systems, a series of single-element simulations was performed. The simulation used a carbon fiber/epoxy material system with various lay-ups, including UD tape and plain-woven fabric variants. This study revealed the elastic-plastic behavior of MAT54, as well as a strong influence of the material strain-to-failure input parameters, rather than the material strength input parameters.

17. Key Words	18. Distribution Statement
Finite element modeling, Damage modeling, Carbon fiber material modeling, LS-DYNA MAT54	This document is available to the U.S. public through the National Technical Information Service (NTIS), Springfield, Virginia 22161. This document is also available from the Federal Aviation Administration William J. Hughes Technical Center at actlibrary.tc.faa.gov.

19. Security Classif. (of this report)	20. Security Classif. (of this page)	21. No. of Pages	22. Price
Unclassified	Unclassified	63	

ACKNOWLEDGEMENTS

This research was performed at the Automobili Lamborghini Advanced Composite Structures Laboratory at the University of Washington. The authors would like to thank Allan Abramowitz, Dr. Larry Ilcewicz, and Joseph Pellettiere (Federal Aviation Administration) for their funding and support of the composite modeling research. Also, the help of the advanced analysis team at the Boeing Company, who were instrumental in establishing the LS-DYNA modeling capabilities at the University of Washington and supporting the ongoing projects concerned with crash simulation, is greatly appreciated.

The authors would also like to thank Dr. Xinran Xiao (previously of General Motors, now at Michigan State University) for his guidance with the fundamentals of explicit finite element modeling, as well as the active members of the Crashworthiness Working Group of the Composite Materials Handbook-17 (CMH-17, formerly MIL-HDBK-17).

TABLE OF CONTENTS

LIST OF FIGURES

LIST OF TABLES

LIST OF SYMBOLS, ACRONYMS, AND MATERIAL PARAMETERS

ε	Strain
σ	Stress
ν	Poisson's ratio
G	Shear modulus
AGATE	Advanced General Aviation Transport Experiment
ALPH	MAT54 parameter: Elastic shear weighting factor
BETA	MAT54 parameter: Shear weighting factor for longitudinal tensile failure
CMH-17	Composite Materials Handbook-17, formerly MIL-HDBK-17
DFAILC	MAT54 parameter: Longitudinal compressive failure strain
DFAILM	MAT54 parameter: Transverse failure strain (both compressive & tensile)
DFAILS	MAT54 parameter: Shear failure strain
DFAILT	MAT54 parameter: Longitudinal tensile failure strain
EA	MAT54 parameter: Longitudinal elastic modulus
EB	MAT54 parameter: Transverse elastic modulus
EFS	MAT54 parameter: Effective failure strain
FBRT	MAT54 parameter: Softening factor for fiber tensile strength after matrix failure
GAB	MAT54 parameter: Shear modulus
PRBA	MAT54 parameter: Minor Poisson's ratio
PW	Plain-weave fabric (composite material system)
SC	MAT54 parameter: Shear strength
SOFT	MAT54 parameter: Softening factor for crushfront elements
TFAIL	MAT54 parameter: Minimum time step size criterion for element deletion
UD	Unidirectional
XC	MAT54 parameter: Longitudinal compressive strength
XT	MAT54 parameter: Longitudinal tensile strength
YC	MAT54 parameter: Transverse compressive strength
YCFAC	MAT54 parameter: Softening factor for fiber compressive strength after matrix failure
YT	MAT54 parameter: Transverse tensile strength

EXECUTIVE SUMMARY

The complex physical nature of the failure modes exhibited by laminated composite materials has made it a great challenge to numerically simulate such material systems beyond the elastic region. Within the state-of-the-art finite element codes used to predict dynamic impact or crash events, composites are modeled as orthotropic linear elastic materials within the failure surface, in which its shape depends on the failure criterion adopted by the specific material model. Beyond the failure surface, the appropriate elastic properties are degraded according to a degradation law. The LS-DYNA material model MAT54 has a history of being used to model composite materials in crash and impact simulations and is of interest for large full-scale structural damage simulations because it is a relatively simple material model that requires minimal input parameters. However, the relative simplicity of MAT54 causes notable shortcomings as a consequence of oversimplification of the complex physical mechanics occurring during failure. Furthermore, MAT54 is specifically designed to simulate unidirectional (UD) tape composite laminates and not fabric materials, although it has been used to model fabric composite material systems in impact simulations.

There is no documentation on MAT54 that fully characterizes the material model and addresses its shortcomings and proper usage. Through the efforts of the Composite Materials Handbook-17 (CMH-17) Crashworthiness Numerical Round Robin, it is evident that in-depth knowledge of composite material models is limited to those with extensive experience; a need for such documentation is apparent. This report contains the results of a single-element investigation, using MAT54 to simulate both a UD tape and a fabric composite material system under simple loading conditions. Parametric studies were performed on each of the MAT54 input parameters to identify sensitive parameters. This report also contains a detailed description of MAT54 and a table of suggested user input parameter definitions.

Results show a great dependency on the material strain-to-failure parameters rather than the strength parameters, even though the failure criteria implemented by MAT54 are strength-based. The strain-to-failure parameters determine element deletion, which is independent of element failure. Elements can be deleted prior to failing if the strain limits are exceeded. Following failure initiation, property degradation is in some cases insignificant, and failed elements can still carry a significant amount of stress until they are deleted. These are all important considerations when defining the material strain-to-failure parameters, which, unlike strengths, are properties not often specified by material data sheets.

Results from the single-element investigation also show that fabric materials can successfully be modeled by MAT54; however, the sensitivity of the user-defined material input parameters on the stress-strain results depends on the loading direction relative to the local material axes when the fabric lay-up is defined uniformly (i.e., all zero direction). In the case of the UD cross-ply laminate, parametric sensitivity studies confirm that the longitudinal (fiber) properties are significantly more influential than the transverse (matrix) properties.

1. INTRODUCTION.

The complex physical nature of the failure modes exhibited by laminated composite materials has made it a great challenge to numerically simulate such material systems beyond the elastic region. In the composites community, it is well accepted that existing failure criteria for composites have several shortcomings, making it a challenge even to predict the onset of damage [1 and 2]. The state-of-the-art finite element codes used to predict the dynamic impact or crash events involving damage, such as LS-DYNA®, ABAQUS/Explicit, RADIOSS®, and PAM-CRASH, implement composite material models created by the software developer to define the elastic, failure, and post-failure behavior of the elements. These material models account for physical properties of the material (e.g., strength, modulus, and strain-to-failure) that can be measured by experiment, but also include software-specific parameters, which either have no physical meaning or cannot be determined experimentally. The current approach requires extensive tuning and calibration of these material models to reach an agreement between experiment and simulation.

Composites are modeled as orthotropic linear elastic materials within the failure surface, in which its shape depends on the failure criterion adopted by the specific material model. Beyond the failure surface, the appropriate elastic properties are degraded according to a model-specific degradation law. Although several codes are available, LS-DYNA has been traditionally considered the benchmark for composite damage simulations and is extensively used in the automotive and aerospace industries to perform explicit dynamic post-failure simulations [3–5]. LS-DYNA contains a number of built-in composite material models, such as MAT22 and MAT54/55, which are progressive damage models that use a ply discount method to degrade elastic material properties, and MAT58, MAT158, and MAT162, which use continuum damage mechanics to define the post-failure material degradation.

The material model MAT54 has been extensively used by the aircraft industry to simulate composite materials undergoing progressive damage under crash conditions as well as foreign object impact scenarios [4–7]. This material model is of interest for large full-scale structural damage simulations because it is a relatively simple material model that requires minimal input parameters. Not only does this reduce the computational requirements of a simulation, it also reduces the difficulty and amount of material testing necessary to generate input parameters. However, the relative simplicity of MAT54 causes notable shortcomings as a consequence of oversimplification of the complex physical mechanics occurring during failure. Furthermore, MAT54 is designed specifically to simulate orthotropic materials with greatly differing properties in the longitudinal and transverse directions, such as unidirectional (UD) composite laminates and not fabric materials. For this reason, it implements a matrix-specific failure criterion in the transverse direction that would not be appropriate to evaluate a fiber-dominated material. Nevertheless, MAT54 has been used to simulate fabric composite structures in crash simulations [4 and 5].

There is no documentation of MAT54 that fully characterizes the material model and addresses its shortcomings and proper usage. The LS-DYNA Keyword User's Manual [8] entry for MAT54 provides little information other than defining the failure criterion and contains several inaccuracies regarding the degradation scheme. Through such efforts as the Composite Materials Handbook -17 (CMH-17) Crashworthiness Numerical Round Robin, it is evident that

the in-depth knowledge of composite material models required for simulation in the elastic-plastic region is limited to those with extensive experience. It has also become apparent that there is a need for better composite material model documentation [1]. This report contains a detailed description of MAT54 and a guide to user input parameter definitions.

To properly use MAT54 in crash and other impact simulations, the shortcomings that arise from the oversimplification of the failure mechanics must be identified and fully understood. Furthermore, the applicability of MAT54 to model a fabric composite material system must be evaluated. To accomplish these tasks, a set of single-element investigations were performed, using MAT54 to simulate a carbon fiber/epoxy material system in both its UD tape and plain-weave fabric (PW) varieties. This report contains the results of the single-element investigation and the results from parametric studies performed on each of the MAT54 input parameters to identify sensitive parameters.

2. LS-DYNA MATERIAL MODEL MAT54.

MAT54 is a progressive failure model that is designed to simulate UD tape composite laminates using shell elements. The LS-DYNA user's manual [8] entry for MAT54 is reproduced in appendix A. To support this discussion, figure 1 shows the entire MAT54 input card with the 43 user-defined inputs grouped into seven color-coded categories. Table 1 provides a list of definitions for all of these parameters and how they are obtained. Appendix B contains suggested values (or ranges of values) for each parameter.

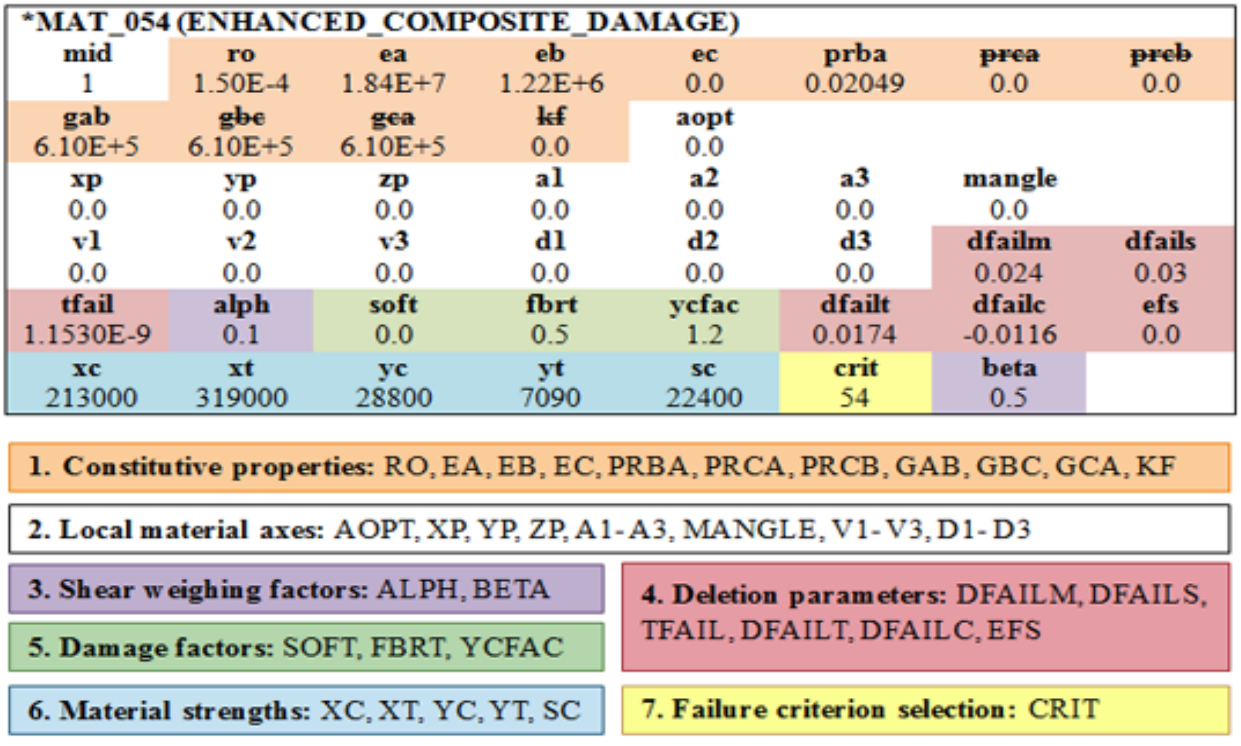

Figure 1. Material Card MAT54 With 43 Parameters Shown in Seven Categories (strikethrough parameters are inactive)

Table 1. MAT54 User-Defined Input Definitions and Required Experimental Data

Name	Definition	Type	Measurement
MID	Material identification number	Computational	N/A
RO	Mass per unit volume	Experimental	Density test
EA	Axial Young's modulus	Experimental	0-degree tension test
EB	Transverse Young's modulus	Experimental	90-degree tension test
EC	Through-thickness Young's modulus	Inactive	
PRBA	Minor Poisson's ratio v_{21}	Experimental	0-degree tension test with biaxial strain measurement
PRCA	Minor Poisson's ratio v_{31}	Inactive	
PRCB	Major Poisson's ratio v_{12}	Inactive	
GAB	Shear modulus G_{12}	Experimental	Shear test
GBC	Shear modulus G_{23}	Inactive	
GCA	Shear modulus G_{31}	Inactive	
KF	Bulk modulus	Inactive	
AOPT	Parameters used to establish the local material axes	Computational	N/A
XP,YP,ZP			
A1,A2,A3			
MANGLE			
V1,V2,V3			
D1,D2,D3			
ALPH	Elastic shear stress nonlinear factor	Shear factor	None
BETA	Shear factor in tensile axial failure criterion	Shear factor	None
DFAILT	Axial tensile failure strain	Experimental	0-degree tension test
DFAILC	Axial compressive failure strain	Experimental	0-degree compression test
DFAILM	Transverse failure strain	Experimental	90-degree tension and compression tests
DFAILS	Shear failure strain	Experimental	Shear test
EFS	Effective failure strain	Optional	None
TFAIL	Time step failure value	Computational	Derived from numeric time step
FBRT	Axial tensile strength factor after 2-direction failure	Damage factor	None
SOFT	Material strength factor after crushing failure	Damage factor	None
YCFAC	Axial compressive strength factor after 2-direction failure	Damage factor	None
XT	Axial tensile strength	Experimental	0-degree tension test
XC	Axial compressive strength	Experimental	0-degree compression test
YT	Transverse tensile strength	Experimental	90-degree tension test
YC	Transverse compressive strength	Experimental	90-degree compression test
SC	Shear strength	Experimental	Shear test
CRIT	Specification of failure criterion	Computational	N/A

MAT54 simulates laminated material systems within a single-shell element by considering each ply in the laminate as an integration point in the two-dimensional element. In the elastic region, the material stress-strain relations are those of Chang and Chang [9], who developed elastic relations specifically for fiber-reinforced laminates in which the fibers are much stiffer than the matrix, such as UD carbon fiber/epoxy laminates. For these types of materials, nonlinear elastic behavior occurs only in the ply shear stresses once they become comparable to longitudinal tensile stresses [9]. The elastic stress-strain relations in each ply for fiber (axial, 1-direction), matrix (transverse, 2-direction), and shear (12-direction) are given by:

$$\varepsilon_{11} = \frac{1}{E_1}(\sigma_{11} - \nu_{12}\sigma_{22}) \tag{1}$$

$$\varepsilon_{22} = \frac{1}{E_2}(\sigma_{22} - \nu_{21}\sigma_{11}) \tag{2}$$

$$2\varepsilon_{12} = \frac{1}{G_{12}}\sigma_{12} + \alpha{\sigma_{12}}^3 \tag{3}$$

The Hahn and Tsai [10] nonlinear shear stress-strain relation is used, and the α (ALPH input parameter in MAT54) term is a weighting factor for the nonlinear shear stress term. The MAT54 ALPH parameter cannot be experimentally determined, but needs to be calibrated by trial and error.

In the plastic region, the LS-DYNA documentation indicates MAT54 as using the Chang-Chang failure criterion; however, only the elastic relations come from these authors. The failure criteria implemented by MAT54 are actually those postulated by Hashin [11], who proposed four separate failure modes of a UD composite laminate under plane stress conditions. Both the Chang-Chang and Hashin failure criteria are derived from the Tsai-Wu [12] interactive stress-based tensor polynomial expression. Whereas Chang and Chang specify only two failure modes (fiber and matrix), Hashin specifies the four modes that are used by MAT54. These four failure modes are represented in MAT54 by the history variables *ef*, *ec*, *em*, and *ed*, which are binary failure flags that represent tension and compression failure in the fiber direction, and tension and compression failure in the matrix direction, respectively.

In the following equations, which define the four MAT54 failure criteria, XT is the fiber tensile strength, XC is the fiber compressive strength, YT is the matrix tensile strength, YC is the matrix compressive strength, and SC is the shear strength of the UD ply. These input parameters can be measured through testing of the UD tape lamina. It should be noted that all of these quantities assume that the 1-direction (axial) is the fiber direction and the 2-direction (transverse) is the matrix direction.

For the tensile fiber mode for which $\sigma_{11} \geq 0$:

$${e_f}^2 = \left(\frac{\sigma_{11}}{x_t}\right) + \beta\left(\frac{\sigma_{12}}{s_c}\right) - 1 \begin{cases} \geq 0 failed \\ < 0 elastic \end{cases} \tag{4}$$

On failure: $E_1 = E_2 = G_{12} = \nu_{12} = \nu_{21} = 0$.

The shear stress weighting factor β (BETA input parameter in MAT54) allows the user to explicitly define the influence of shear in the tensile fiber mode. This is the only alteration of the original Hashin failure criterion in MAT54, where BETA = 1, the Hashin fiber tension criterion is implemented, and setting BETA = 0 reduces equation 4 to the Maximum Stress failure criterion. Selecting the BETA value is a matter of preference and can be done by trial and error.

For the compressive fiber mode where $\sigma_{11} < 0$:

$$e_c{}^2 = \left(\frac{\sigma_{11}}{X_c}\right)^2 - 1 \begin{cases} \geq 0 failed \\ < 0 elastic \end{cases} \tag{5}$$

On failure: $E_1 = \nu_{12} = \nu_{21} = 0$.

For the tensile matrix mode where $\sigma_{22} \geq 0$:

$$e_m{}^2 = \left(\frac{\sigma_{22}}{Y_t}\right)^2 + \left(\frac{\sigma_{12}}{s_c}\right)^2 - 1 \begin{cases} \geq 0 failed \\ < 0 elastic \end{cases} \tag{6}$$

On failure: $E_2 = \nu_{21} = G_{12} = 0$.

For the compressive matrix mode where $\sigma_{22} < 0$:

$$e_d{}^2 = \left(\frac{\sigma_{22}}{2S_c}\right)^2 + \left[\left(\frac{Y_c}{2S_c}\right)^2 - 1\right]\frac{\sigma_{22}}{Y_c} + \left(\frac{\sigma_{12}}{s_c}\right)^2 - 1 \begin{cases} \geq 0 failed \\ < 0 elastic \end{cases} \tag{7}$$

On failure: $E_2 = \nu_{12} = \nu_{21} = G_{12} = 0$.

When one of the above conditions is exceeded in a ply within the element, the specified elastic properties for that ply are set to zero. The mechanism by which MAT54 applies this elastic property reduction simply prevents the failed ply from carrying increased stress, rather than reducing the stress to zero or a near-zero value. The incremental formulation used by MAT54 to determine 1- and 2-direction element stresses in the i^{th} time step provides insight into this mechanism:

$$\begin{bmatrix}\sigma_{11} \\ \sigma_{22}\end{bmatrix}_i = \begin{bmatrix}\sigma_{11} \\ \sigma_{22}\end{bmatrix}_{i-1} + \begin{bmatrix}c_{11}\ c_{11} \\ c_{22}\ c_{22}\end{bmatrix}_i \begin{bmatrix}\Delta\varepsilon_{11} \\ \Delta\varepsilon_{22}\end{bmatrix}_i \tag{8}$$

When ply failure occurs in the i^{th} time step, constitutive properties in the stiffness matrix (C) are set to zero, but the stresses from the i^{-1} time step are nonzero. This leads the failed ply stresses to be constant and unchanged from the stress state just prior to failure. Figure 2 shows the resulting plastic behavior, which occurs when the ply strength (F^u) is reached before the failure strain (DFAIL). Elastic property degradation following failure in MAT54 works in this way, rather than degrading properties in the elastic equations (equations 1 through 3), which would result in a reduced- or zero-stress state in a failed ply.

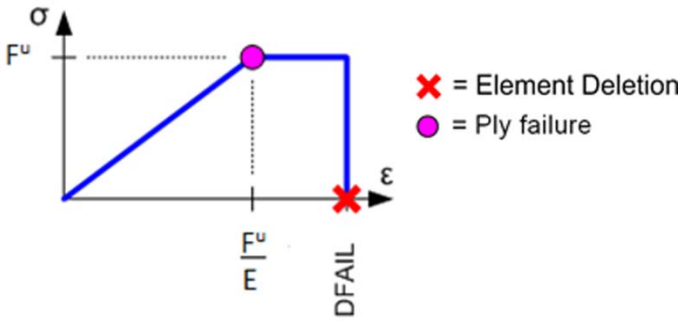

Figure 2. Elastic-Plastic Stress-Strain Behavior of MAT54

The MAT54 FBRT and YCFAC strength-reduction parameters are used to degrade the pristine fiber strengths of a ply if compressive matrix failure takes place (equation 7). This strength reduction simulates damage done to the fibers from the failed matrix. It is applied using:

$$XT = XT^* * FBRT \tag{9}$$

$$XC = YC^* * YCFAC \tag{10}$$

where the asterisk denotes the initial, pristine value of the input parameter as defined by the user.

The FBRT parameter defines the fraction of the pristine fiber strength that is left following failure; therefore, its value should be in the range [0,1]. The YCFAC parameter uses the pristine matrix strength YC to determine the damaged compressive fiber strength; therefore, the upper limit of YCFAC is XC/YC. The input value for the two parameters FBRT and YCFAC cannot be measured experimentally and must be determined by trial and error.

The SOFT parameter is a strength-reduction factor used specifically for crush simulations [13]. This parameter reduces the strength of the elements immediately ahead of the crush front to simulate damage propagating from the crush front. The strength degradation is applied to four of the material strengths as follows:

$$\{XT, XC, YT, YC\} = \{XT, XC, YT, YC\}^* * SOFT \tag{11}$$

where the asterisk indicates the pristine strength value.

Reducing material strengths using SOFT allows for greater stability to achieve stable and progressive crushing by softening the load transition from the active row of elements to the next. The SOFT parameter is active within the range [0 to 1], where SOFT = 1 indicates that the elements at the crush front retain their pristine strength and no softening occurs. Because this parameter cannot be measured experimentally, it must be calibrated by trial and error for crush simulations.

The failure equations described in equations 4–7 provide the maximum stress limit of a ply, and the damage mechanisms described in equations 9–11 reduce the stress limit by a specified value, given specific loading conditions. However, none of these mechanisms cause the ply stress to go to zero. Instead, there are five critical strain values that reduce the ply stresses to zero. These

include the four strain-to-failure values that can be measured using coupon-level tests in the positive fiber direction (tension) DFAILT, in the negative fiber direction (compression) DFAILC, in the matrix direction DFAILM, and in shear DFAILS. It is important to note that in the matrix direction there is only one modulus and one failure strain value that is used for both tension and compression and that, experimentally, these values are often different. The fifth critical strain parameter is a nonphysical failure strain parameter called the effective failure strain (EFS) and is given by:

$$EFS = \sqrt{\frac{4}{3}(\varepsilon_{11}{}^2 + \varepsilon_{11}\varepsilon_{22} + \varepsilon_{22}{}^2 + \varepsilon_{12}{}^2)} \tag{12}$$

A critical EFS value can be calculated by experimentally determining 1-, 2-, and 12-strains at failure and using them in equation 12. This equation effectively defines a mixed-mode, strain-based deletion surface that reflects multiaxial loading. Defining EFS values in MAT54 below the critical experimental value would cause premature element deletion. The default value for EFS is zero, which is interpreted by MAT54 to be numerically infinite.

In MAT54, a ply strain that exceeds the appropriate DFAIL parameter causes ply stresses to immediately reduce to zero. An element is deleted once the stress in all of the plies has been reduced to zero; therefore, these DFAIL parameters directly influence MAT54 element deletion.

Element deletion can also occur when the element becomes highly distorted and requires a very small time step. A minimum time step parameter, TFAIL, removes distorted elements as follows:

TFAIL ≤ 0: No element deletion by time step

$0 <$ TFAIL ≤ 0.1: Element is deleted when its time step is smaller than TFAIL

TFAIL > 0.1: Element is deleted when $\frac{\text{Current time-step}}{\text{Original time-step}} <$ TFAIL

Element deletion due to a time-step restriction is purely a computational function that can reduce the computational cost of a highly distorted simulation and should not be relied on as a means for primary element deletion. If significant element distortion is not a concern, choosing a value that is two orders of magnitude smaller than the element time step for TFAIL is recommended. Defining TFAIL to be very near or greater than the element time step would cause premature element deletion because the element would violate the TFAIL condition near its initial state.

Unlike the strength-based ply failure criteria in equations 4–7, there are no history variables for ply failure due to maximum strains or element deletion caused by TFAIL. For this reason, it is not possible from the simulation results to identify the condition that caused element deletion.

3. SINGLE-ELEMENT SIMULATIONS.

3.1 MODEL SETUP.

The MAT54 material model was used to simulate a T700/2510 carbon fiber/epoxy prepreg in both the UD tape and PW variants. The material properties of both the UD and PW forms are well documented as part of the Advanced General Aviation Transport Experiment (AGATE) Program [14 and 15] sponsored by the Federal Aviation Administration, and are reproduced in table 2. Appendix C provides the MAT54 input cards from the baseline models for both material systems.

To characterize the basic MAT54 material model elastic, failure initiation, and post-failure behavior, single-shell elements simulating simple UD $[0]_{12}$ and $[90]_{12}$ lay-ups were modeled, for which the material response could be easily anticipated given material properties in table 2. Because all of the plies are in a single direction for these lay-ups, the simulated ply response was the same as the laminate response, and first-ply failure corresponded to laminate failure.

To evaluate the suitability of MAT54 to model fabric material systems, a simple $[(0/90)]_{8f}$ lay-up PW material was used. The simulated results of the fabric material modeled in a single element were compared to those obtained from modeling a comparable UD laminate, which experimentally has similar properties to the fabric laminate, a UD cross-ply $[0/90]_{3s}$.

Table 2. Material Properties Provided by the AGATE Design Allowables for T700GF 12k/2510 UD Tape and T700SC 12k/2510 PW Fabric

Parameter	Property	UD	PW
P (g/cc)	Density	1.51–1.57	1.48–1.5
F_1^{tu} (ksi)	Longitudinal Tensile Strength	319	132
E_1^t (Msi)	Longitudinal Tensile Modulus	18.1	8.11
v_{12}	Major Poisson's Ratio	0.309	0.043
F_2^{tu} (ksi)	Transverse Tensile Strength	7.09	112
E_2^t (Msi)	Transverse Tensile Modulus	1.22	7.96
F_1^{cu} (ksi)	Longitudinal Compressive Strength	210	103
E_1^c (Msi)	Longitudinal Compressive Modulus	16.3	8.09
F_2^{cu} (ksi)	Transverse Compressive Strength	28.8	102
E_2^c (Msi)	Transverse Compressive Modulus	1.47	7.77
F_{12}^{su} (ksi)	Shear Strength	22.4	19.0
G_{12}^s (Msi)	Shear Modulus	0.61	0.609

The ply angles and thicknesses were defined at each integration point in the *PART_COMPOSITE input card. From the coupon-level material tests of these laminates that were conducted at the University of Washington, the average laminate thicknesses were

measured to be 0.079 inch (2.0 mm) and 0.073 inch (1.9 mm) for the 12-ply UD and 8-ply PW laminates, respectively.

A single square element for each laminate was subjected to tension and compression loading in the axial direction, as shown by the schematic of loading and boundary conditions in figure 3. The element used was an LS-DYNA Type 16 fully integrated shell element with an edge length (mesh size) of 0.1 inch (2.5 mm). The *z*-direction displacement on all nodes was constrained. A constant loading rate of 2 in/s (51 mm/s) was applied to nodes 1 and 4 of the single element. The time step was chosen to be 50% of the critical time step, which is the maximum value determined by the Courant condition [16]. Therefore, the baseline time step was 2.846E-7 seconds. It was necessary to use a double-precision solver for the single-element simulations to avoid some instabilities.

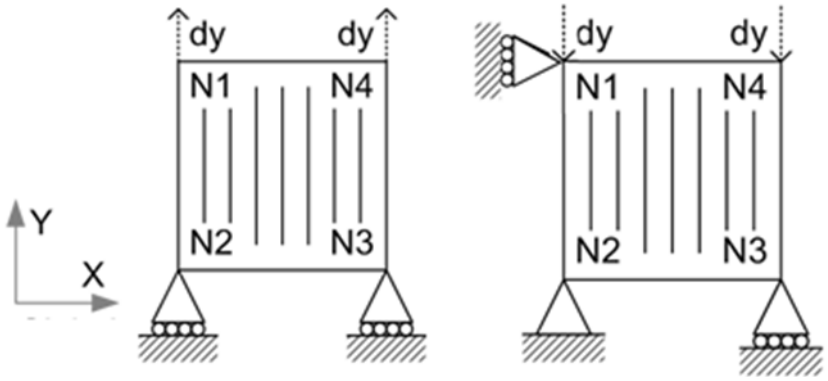

Figure 3. Schematic of the Single Element MAT54 Simulations for Tension (left) and Compression (right) Load Cases

Whereas most of the MAT54 input parameters can be determined from the published material data given in table 2, the AGATE design allowables report does not include strain to failure values [14 and 15]. Instead, the AGATE report suggests the use of simple one-dimensional linear stress-strain relationships to obtain corresponding failure strain values. Whereas this is a valid approximation for fiber-dominated laminates, a nonlinear response is expected for matrix-dominated laminates (such as $[90]_{12}$). Regardless, the design allowable guidelines were followed, and the MAT54 failure strain parameters were calculated by dividing the material strength by the appropriate modulus as follows:

$$\text{DFAILT} = \frac{XT}{EA} \tag{13}$$

$$\text{DFAILC} = \frac{XC}{EA} \tag{14}$$

$$\text{DFAILM} = \frac{YT}{EB} \tag{15}$$

$$\text{DFAILM} = \frac{YC}{EB} \tag{16}$$

where DFAILM can be defined by equations 15 or 16 using either the tensile or compressive matrix strengths. Because DFAILM defines the failure strain for both loading conditions, the higher of the two values from equations 15 or 16 is recommended to define DFAILM, which often provides better stability. Both DFAILM calculations were investigated in the single-element parametric study.

The baseline MAT54 input parameter values for both material systems are presented in table 3, which does not include inactive parameters or those that establish the local material axes (see table 1). For each laminate and loading condition, parametric studies were performed by varying the 20 MAT54 input parameters in table 3. For the simple uniaxial loading conditions, many of the MAT54 parameters were found to have insignificant or no influence on the simulation outcome. These included shear parameters, ALPH, BETA, DFAILS, GAB, and SC, as well as parameters that require special loading conditions to activate, such as SOFT, FBRT, and YCFAC. Finally, the Poisson's ratio, PRBA, had a negligible effect on the results. None of these parameters are discussed in the result sections. The investigation of the EFS and TFAIL input parameters found that these two deletion parameters were not uniquely influential among the single elements investigated and that they provide a utility that can be applied to any laminate and loading condition. The parametric results for these two parameters are discussed in section 3.2.3.

Table 3. MAT54 Parameters, Baseline and Investigated Values

MAT54 Parameter	Baseline UD Value	Baseline PW Value
EA (Msi)	18.1	8.11
EB (Msi)	1.22	7.89
GAB (Msi)	*.61*	*.609*
PRBA	*0.02049*	*0.043*
XT (ksi)	319	132
XC (ksi)	210	103
YT (ksi)	7.09	112
YC (ksi)	28.8	102
SC (ksi)	22.4	19
DFAILT (in/in)	0.0174	0.0164
DFAILC (in/in)	-0.0116	-0.0127
DFAILM (in/in)	0.024	0.014
DFAILS (in/in)	*0.03*	*0.03*
EFS (in/in)	0	0
TFAIL (sec)	1.153E-9	1.153E-9
FBRT	*0.5*	*0.5*
YCFAC	*1.2*	*1.2*
SOFT	*0*	*0*
ALPH	*0.1*	*0.1*
BETA	*0.5*	*0.5*

Note: Italicized parameters were not applicable to the parametric study of MAT54 parameters.

As a part of this research, loading velocities from 1 in/min (25 mm/min) to 300 in/s (7.6 m/s) were simulated for every element, and results remained unchanged throughout the velocity range. Because MAT54 does not have any strain-rate sensitive parameters and inertial effects are suppressed by the displacement boundary conditions applied to the nodes, this result was expected and is not discussed in the result sections.

For all of the single-element simulations, data were generated at three levels of scale: (1) at the integration point (ply), (2) at the node, and (3) at the element (laminate). Data were recorded in all directions; however, for the purpose of this study, only relevant data in the loading direction were reported. Data of interest at each integration point were the ply stresses and strains. Reaction forces at the boundary conditions on nodes 2 and 3 were recorded to generate the equivalent stress-strain data for the element and verify reported element results. Displacements and velocities were recorded on the free node (node 4), to monitor for unstable behavior. Finally, the total energy of the element was recorded. History variables (equations 4–7) were monitored at the ply and element levels. Because history variables report only stress-based failures, the data were not found to be particularly useful because many important MAT54 behaviors are strain based.

Modeling parameters that were capable of significantly changing the stress-strain behavior, energy, or stability of the simulation are discussed in section 3.2.3. Each laminate was first simulated using the MAT54 input values found in table 3. These initial simulations provided baseline numeric data against which data from the parametric studies were compared.

3.2 UNIDIRECTIONAL $[0]_{12}$ AND $[90]_{12}$ LAMINATES.

3.2.1 Expected Results.

Given the material strengths and properties for the UD material system in table 2, the expected stress-strain responses of the UD $[0]_{12}$ and UD $[90]_{12}$ elements were generated using the linear elastic equations 1 and 2 and the same failure criterion as MAT54, assuming no shear. The energy output was determined by calculating the area under the linear force-displacement curve. Force was calculated by multiplying the stress by the cross-sectional area of the element, and displacement was calculated by multiplying the strain by the element length.

The stress-strain results were compared against experimental coupon tests of the UD laminates performed at the University of Washington. Figure 4(a) shows the results from the $[0]_{12}$ coupon tests, which align well with the expected linear elastic results. Figure 4(b) shows the $[90]_{12}$ experimental results, which deviate from the calculated linear stress-strain curve. Because nonlinear behavior is characteristic of matrix-dominated laminates, deviations from the linear elastic assumption were anticipated.

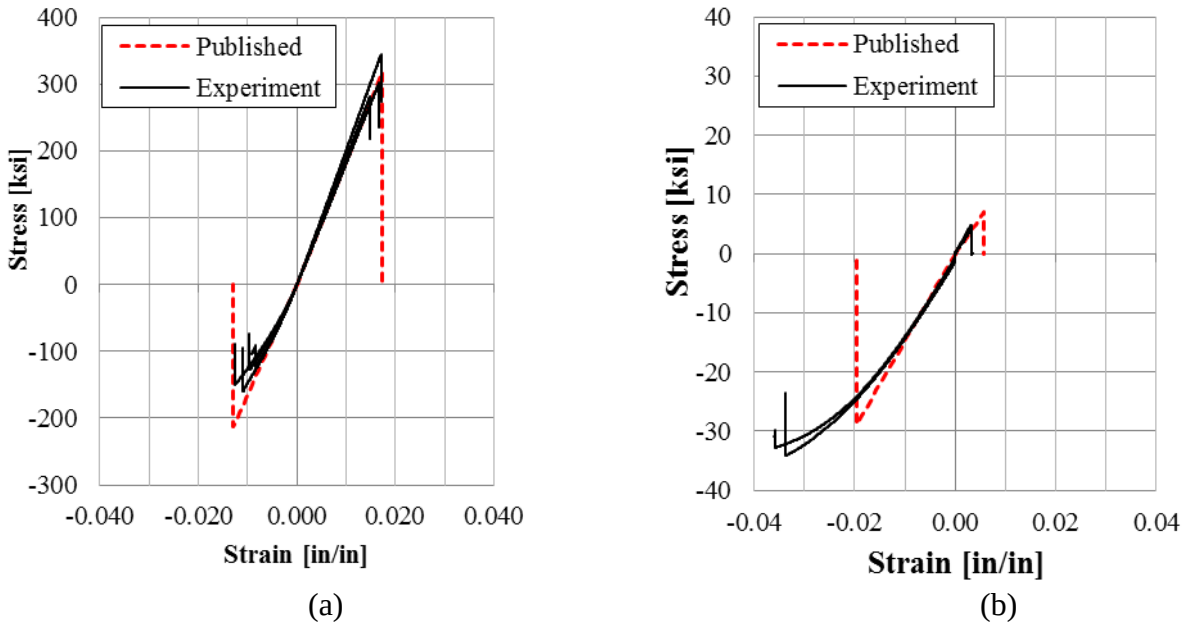

Figure 4. Stress-Strain Curves From (a) $[0]_{12}$ and (b) $[90]_{12}$ Quasistatic Coupon Tests and the Published Material Data From References 14 and 15

3.2.2 Baseline Simulation Results.

The $[0]_{12}$ UD single element was loaded along the fiber direction and produced the stress-strain curve shown in figure 5a. These results correlated perfectly with the expected linear elastic curve. Parabolic behavior was observed in the output energy plot, as shown in figure 5(b), with a total strain energy result of 0.25J at failure under tensile loading without error against the expected result. Table 4 compares the strengths, failure strains, and output energies for the $[0]_{12}$ and $[90]_{12}$ laminates expected from the linear theory against those generated by the simply loaded MAT54 single elements.

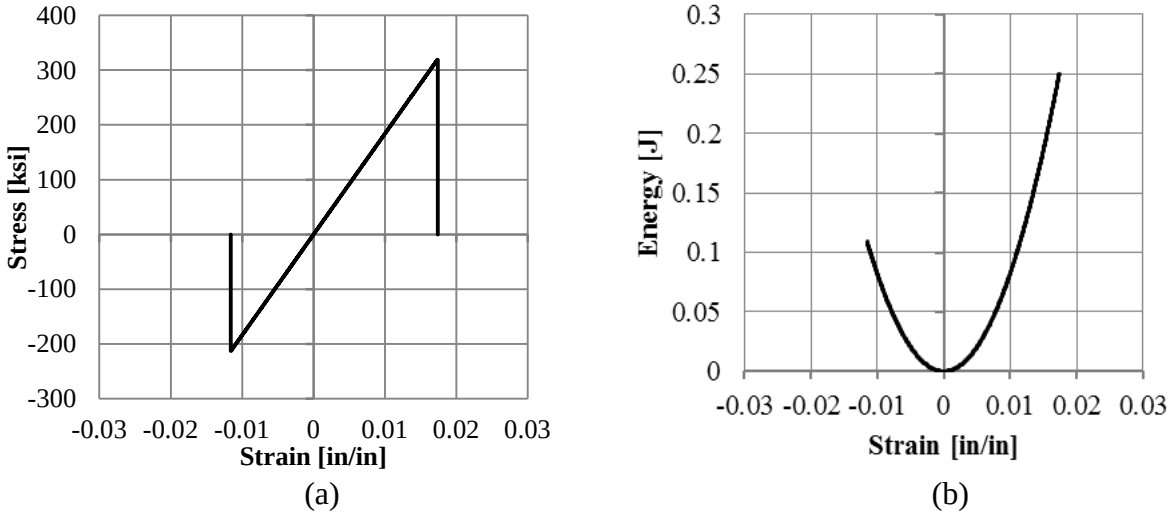

Figure 5. Laminate (a) Stress-Strain and (b) Output Energy Curves for the Baseline $[0]_{12}$ Single-Element Simulation

Table 4. Expected Baseline Strength, Failure Strain, and Output Energy Values for the AGATE UD Material System Compared With the Baseline Single-Element Model Results

Parameter	Expected Result	MAT54 Baseline	Error
F_1^{tu}	319 ksi	319 ksi	0.0%
F_2^{tu}	7.09 ksi	7.09 ksi	0.0%
F_1^{cu}	-213 ksi	-213 ksi	0.0%
F_2^{cu}	-28.8 ksi	-28.8 ksi	0.0%
ε_1^{tu}	0.01734 in/in	0.01738 in/in	0.3%
ε_2^{tu}	0.00581 in/in	0.02399 in/in	313%
ε_1^{cu}	-0.01158 in/in	-0.01158 in/in	0.0%
ε_2^{cu}	-0.02361 in/in	-0.02398 in/in	1.6%
Energy_1^{t}	0.2468J	0.2501J	1.3%
Energy_2^{t}	0.00184J	0.01351J	635%
Energy_1^{c}	0.1100J	0.1095J	0.5%
Energy_2^{c}	0.03034J	0.03083J	1.6%

Predictions for the simulation of the UD laminate loaded in the matrix direction were not as successful. Simulation results in compression correlated very well with expected results, both for stress and energy; however, in tension, the MAT54 results did not match expectations. Figure 6(a) shows the unexpected, perfectly plastic region following the linear elastic behavior in tension. This plastic region was a consequence of the way MAT54 computes the element stresses after failure using equation 8, as shown in figure 2, and the lacking capability to enter two separate failure strain values in the material card for tension and compression in the transverse direction.

As previously noted in section 2.0, there is only one modulus and one failure strain parameter in the matrix direction, meaning the tensile and compressive values cannot be independently defined. As a consequence, only one strength value can satisfy the linear elastic relationship between stress and strain, but there are two matrix strength parameters for tension and compression. Because these strengths are different and the matrix failure strain was determined using compressive value equation 16, the tensile loading case will not satisfy the linear elastic stress-strain relationship of equation 15. Thus, the simulation reached the tensile strength before the matrix failure strain and continued to plastically strain and carry stress until the failure strain (0.024 in/in) was reached. This strain value was more than four times greater than the expected strain at failure. The plasticity caused the energy to increase linearly, which added a significant amount of energy to the output of the baseline simulation (figure 6b). The MAT54 simulation of the UD matrix in tension did not agree with the expected behavior and already demonstrates the importance of the MAT54 failure strain parameters.

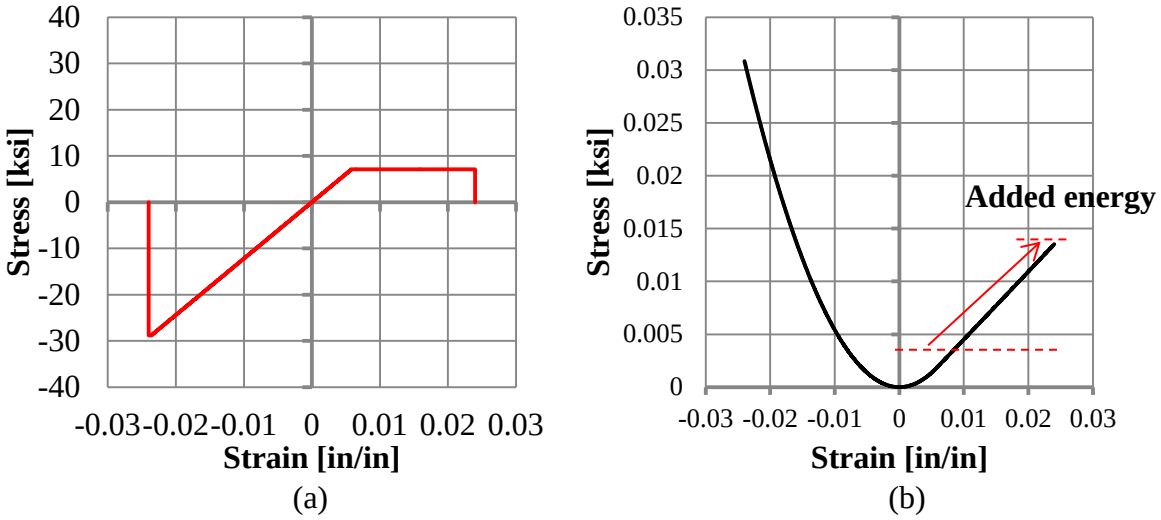

Figure 6. MAT54 Results for Baseline $[90]_{12}$ Laminate (a) Stress-Strain and (b) Energy (with added energy highlighted)

3.2.3 Results From the UD $[0]_{12}$ Laminate Parametric Study.

Table 5 shows the test matrix for the study of MAT54 parameters using the UD $[0]_{12}$ laminate. The parameters that exclusively influenced the matrix direction, such as EB, DFAILM, YC, and YT, are omitted from this report because they were found to have no influence on the $[0]_{12}$ simulations in the loading direction.

Table 5. Parametric Test Matrix for the MAT54 UD $[0]_{12}$ Laminate

Parameter	Baseline Value	Parametric Value				
EA (Msi)	18.1	0	92	378	----	----
XT (ksi)	314	0	200	400	----	----
XC (ksi)	210	0	50	100	200	300
DFAILT (in/in)	0.0174	0	0.01	0.03	----	----
DFAILC (in/in)	-0.0116	0	-0.005	-0.01	-0.02	-0.03
EFS (in/in)	0	0.001	0.01	0.017821	----	----
TFAIL (sec)	1.153E-9	2.835E-7	2.840E-7	2.846E-7	----	----

Changing the fiber modulus, EA, affected the single element both in tension and compression because MAT54 does not distinguish compressive and tensile moduli. As expected, larger values of EA produced a stiffer stress response from the single element, and lower EA values produced a softer response (figure 7). The failure strain remained the same when changing EA, causing the element with a low modulus to fail at a lower stress value. For the high modulus case, the stress stopped increasing at the strength value and remained at that level while plastically deforming until the failure strain was reached and the element was deleted. Because this was a fiber-dominated laminate, the plastic response from the high modulus case was not expected and is not physically meaningful.

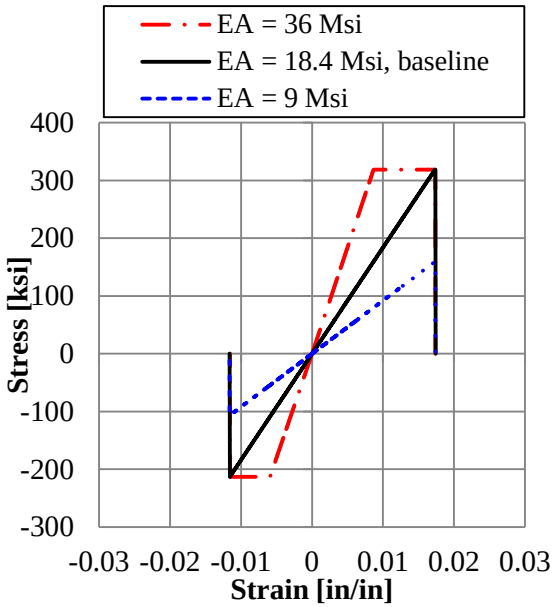

Figure 7. Stress-Strain Results From Changing the Fiber Modulus, EA in UD $[0]_{12}$ Laminate

Figure 8 shows element stress-strain plots for parametric studies of the fiber strengths: XT for tension and XC for compression. Increasing the strength input values larger than the baseline values did not change the results from the baseline. For these simulations, the ply strains exceeded their failure values (DFAIL) before the increased strength was achieved and element deletion occurred. Material strengths set to zero are considered by MAT54 to be numerically

infinite, such that the zero-value simulations produced the same results as simulations with increased strengths. Lowering the fiber strengths below the baseline value lowered the peak stress limit of the element; however, the stress remained constant after achieving this limit and continued straining until the element was deleted at the failure strain. Because a MAT54 element remains intact until achieving the failure strain, raising and lowering the strength input values did not achieve the results expected of a linear elastic material model using stress-based failure criteria. The great dependence of MAT54 on the strain parameters, rather than the strength parameters, was instead demonstrated, as well as the elastic-plastic behavior of a failed MAT54 element.

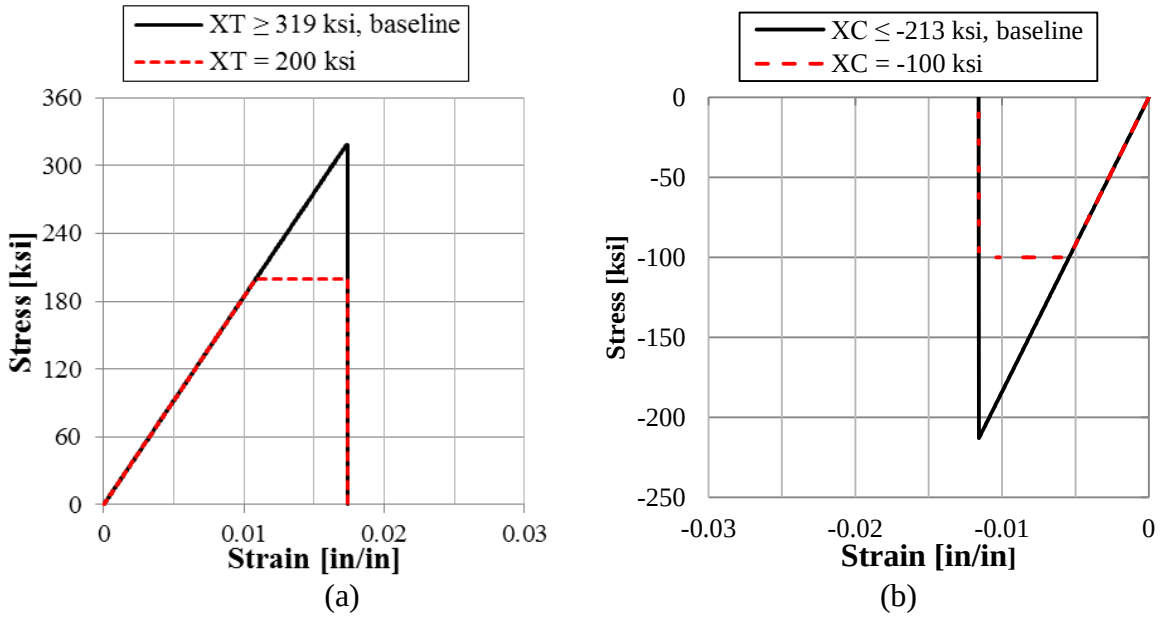

Figure 8. Stress-Strain Curves Resulting From Changing the MAT54 Parameters for Fiber Strength in (a) Tension (XT) and (b) Compression (XC) in UD $[0]_{12}$ Laminate

To demonstrate the difference between expected results and the results given by MAT54 when plasticity is present, a simulation with plasticity in both tension and compression was generated by lowering the XT and XC strengths by approximately 100 ksi. The resulting laminate stress-strain curve with plasticity is plotted in figure 9a, along with the baseline curve and the expected brittle stress-strain result. In figure 9b, the total energy outputs from these three cases are plotted. Following stress failure and in the plasticity region, energy increased linearly until the failure strain was reached. From this plastic energy growth, a laminate with a 100 ksi strength reduction had only an 18% loss in strain energy at element deletion. The MAT54 energy output was more than two times greater than what was expected.

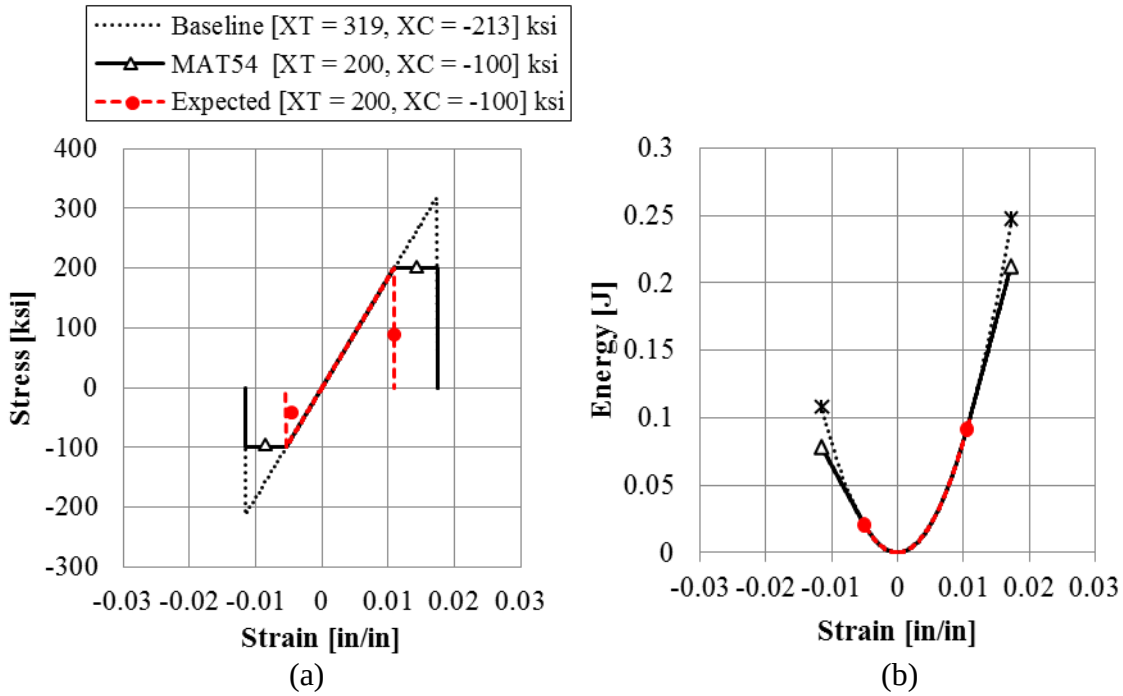

Figure 9. Expected Results and the MAT54 Results When the Strength Is Reduced by 100 ksi: (a) Stress-Strain and (b) Output Energy in UD $[0]_{12}$ Laminate

Figure 10 shows element stress-strain plots for parametric studies of the fiber failure strain parameters, DFAILT for tension, and DFAILC for compression. Increasing these values larger than the baseline caused perfect plasticity along the ultimate stress value until the increased failure strain value was reached. Decreasing the failure strains caused early element deletion before the ultimate material strength was reached. For simulations with especially large plastic zones, such as DFAILC = -0.03 in/in, it was necessary to decrease the time step to simulate the large deformation and avoid minor instabilities.

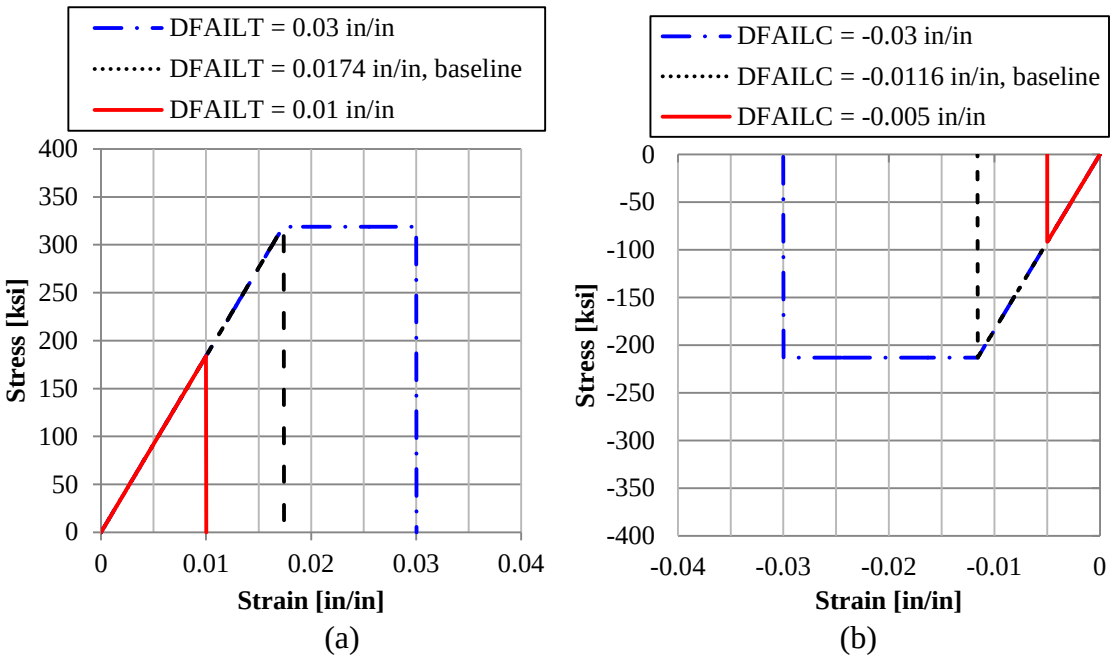

Figure 10. Stress-Strain Curves Resulting From Changing the MAT54 Parameters for Fiber Failure Strain in (a) Tension (DFAILT) and (b) Compression (DFAILC) in UD $[0]_{12}$ Laminate

A simulation with plasticity in both tension and compression was generated by using failure strains of ±0.03 in/in. Figure 11 shows the resulting laminate stress-strain and energy curves with the expected linear elastic curves.

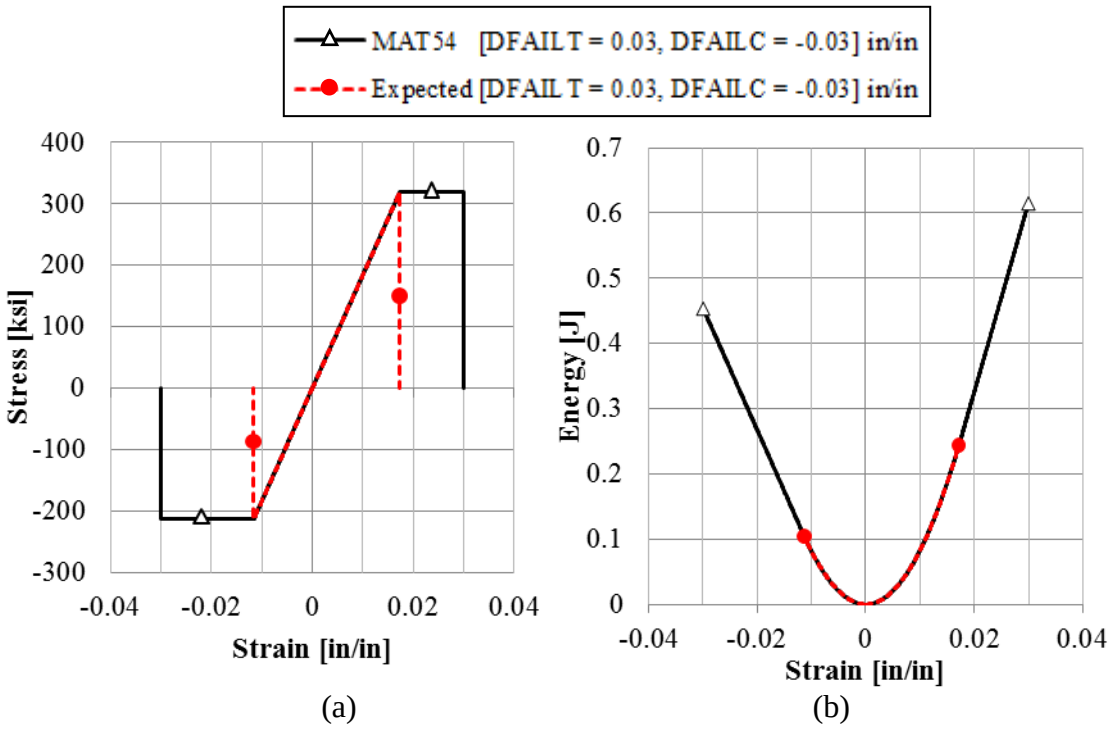

Figure 11. Expected Results and the MAT54 Results When the Failure Strain Is Increased to ±0.03 in/in: (a) Stress-Strain and (b) Output Energy in UD $[0]_{12}$ Laminate

With these increased failure strains, the simulated MAT54 energy was three times the total energy expected from linear elastic behavior. Whereas the effect on the shape of the stress-strain curve from changing the failure strains resembled that from changing the material strengths, the plasticity caused by varying failure strains produced a greater error in energy. With decreased strengths, the magnitude of the energy added was relatively lower because the added plasticity occurred at a value below the material strength. However, adding plasticity by increasing the failure strain added energy at a greater rate because the added plasticity occurred at the ultimate material strength.

A special case arose when DFAILT was set to zero. Without the fiber tension failure strain to determine element deletion, the fiber tensile strength, XT, initiated element deletion. When the element failed in the fiber tension mode, MAT54 implemented a special degradation scheme for the ply stresses, which reached zero in exactly 100 time steps, and the element was deleted. Figure 12 shows in the stress-strain plot the degradation of the element stress when DFAILT = 0. Although this failure mode more closely resembles the desired linear elastic behavior of a UD laminate, this special case was applicable only to DFAILT and did not work for DFAILC or DFAILM. For example, using DFAILC ≥ 0 immediately terminated the simulation because the maximum failure strain was violated upon initiation of the simulation. Furthermore, when DFAILT was set to zero, but the loading case was not tension in the fiber direction (e.g., fiber compression, matrix tension, matrix compression), the special case shown in figure 12 did not apply. This is not a realistic MAT54 failure mode on which to rely because it requires very particular loading conditions.

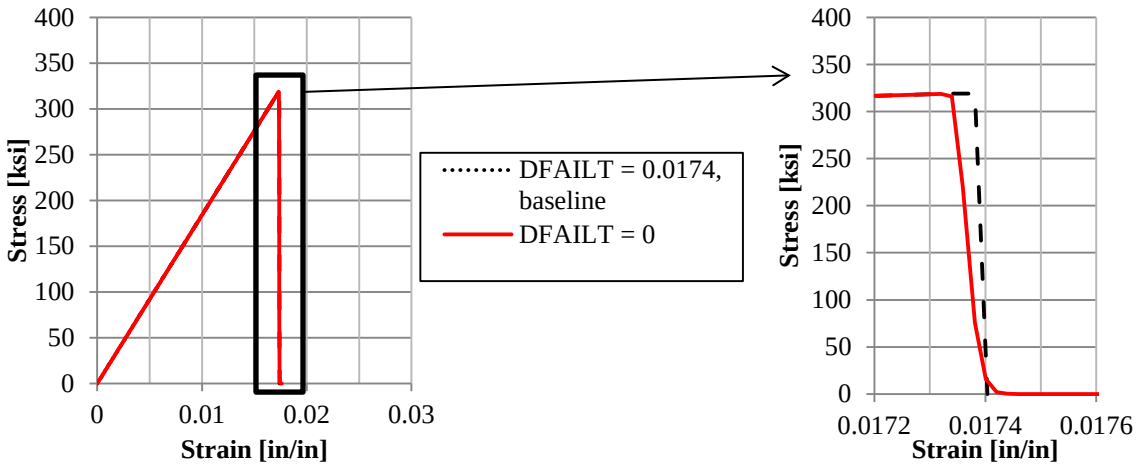

Figure 12. Stress-Strain Results Showing Stress Degradation When DFAILT = 0 in UD $[0]_{12}$ Laminate in Tension

Determining the effect of the EFS parameter required that the critical EFS value for this material system be determined. This was done by using the 1-, 2-, and 12-strains at failure in equation 12. The resulting critical EFS value was 0.0178 in/in. Using an EFS value less than the critical value caused the element to be deleted earlier than the baseline, as shown in figure 13. Implementing values higher than the critical value did not change the results because the DFAILT parameter controlled element deletion rather than EFS. The default value of EFS is zero, which MAT54 considers numerically infinite.

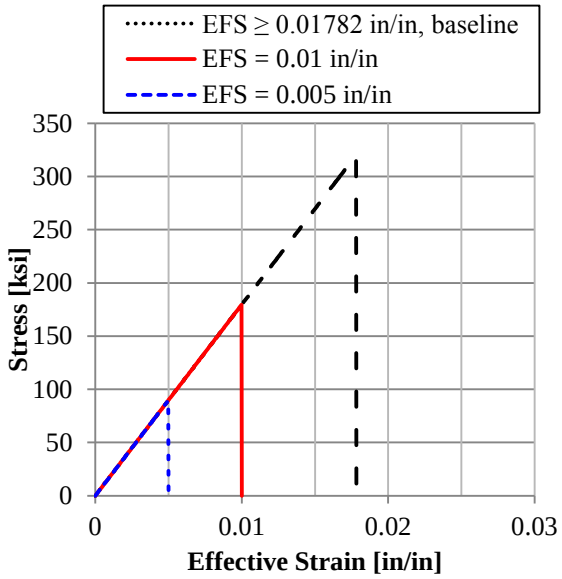

Figure 13. Stress vs. Effective Strain Results From the EFS Parameter Study in UD $[0]_{12}$ Laminate

Finally, altering TFAIL so it was greater than the element time step caused early element deletion. This effect can be seen only by using TFAIL values slightly larger than the element

time step (figure 14). Implementing values larger than this eliminated the element at the onset of the simulation. A value that was two orders of magnitude smaller than the element time step was chosen for the baseline to prevent errors. It should be stressed that element deletion due to TFAIL is purely a computational function that reduces the computational time of a highly distorted simulation and should not be relied on as a means for primary element deletion.

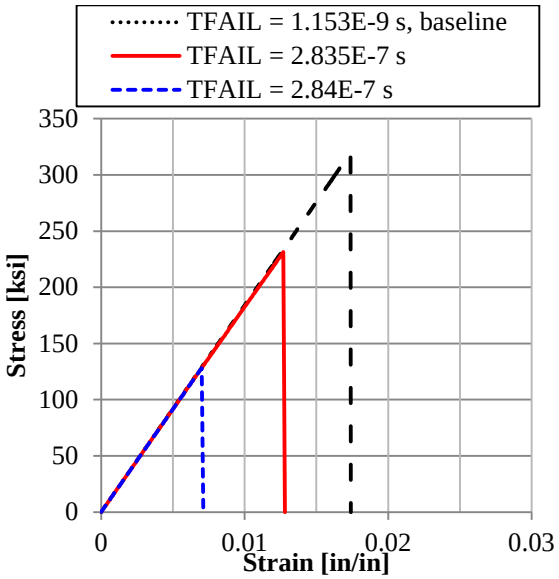

Figure 14. Stress vs. Strain Results From the TFAIL Parameter Study in UD $[0]_{12}$ Laminate

3.2.4 Results From the UD $[90]_{12}$ Laminate Parametric Study.

Table 6 shows the test matrix for the UD $[90]_{12}$ parametric study. The test matrix was reduced by excluding parameters that exclusively influence the fiber direction, such as EA, DFAILT, DFAILC, XT, and XC, none of which were observed to affect the $[90]_{12}$ simulations in the loading direction.

Table 6. Parametric Test Matrix for the MAT54 UD $[90]_{12}$ Laminate, Baseline and Investigated Values

Parameter	Baseline Value	Parametric Value					
EB (Msi)	1.22	0	.61	18.3	----	----	----
YT (ksi)	7.09	0	3.545	25	29.28	40.00	----
YC (ksi)	28.8	0	14.4	21.6	40.00	----	----
DFAILM (in/in)	0.024	0	0.00291	0.00581	.012	.02361	0.035

As expected, changing the matrix modulus, EB, had the same effect on the UD $[90]_{12}$ laminate as changing the fiber modulus in the UD $[0]_{12}$ laminate. Raising EB caused a stiffer stress response and lowering it caused a softer response, both in tension and compression (figure 15).

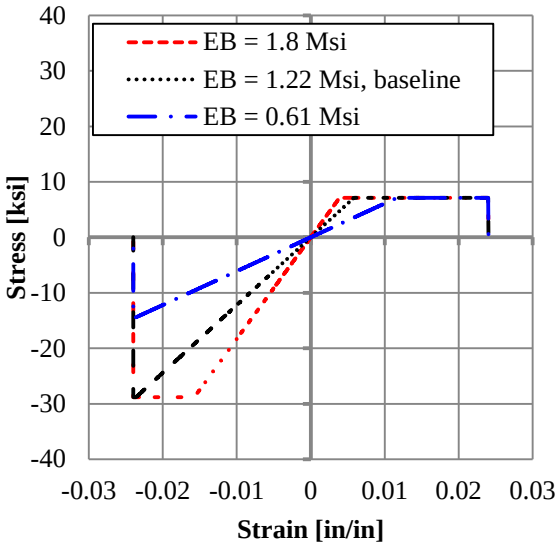

Figure 15. Stress-Strain Results From Changing the Matrix Modulus EB in UD $[90]_{12}$ Laminate

The matrix strengths, YT for tension and YC for compression, determined the peak stress limits of the $[90]_{12}$ single element, and the effect of these strengths was similar to the effect of the fiber strengths on the $[0]_{12}$ element. Strength values greater than or equal to 28.8 ksi for both YT and YC caused perfectly linear elastic stress-strain behavior. This strength threshold was determined from the linear elastic stress-strain relation given in equation 16. As shown in figure 16, strength values less than 28.8 ksi caused failure, followed by a region of constant stress, until the failure strain was reached and the element deleted. A zero value for either strength parameter was considered by MAT54 to be numerically infinite.

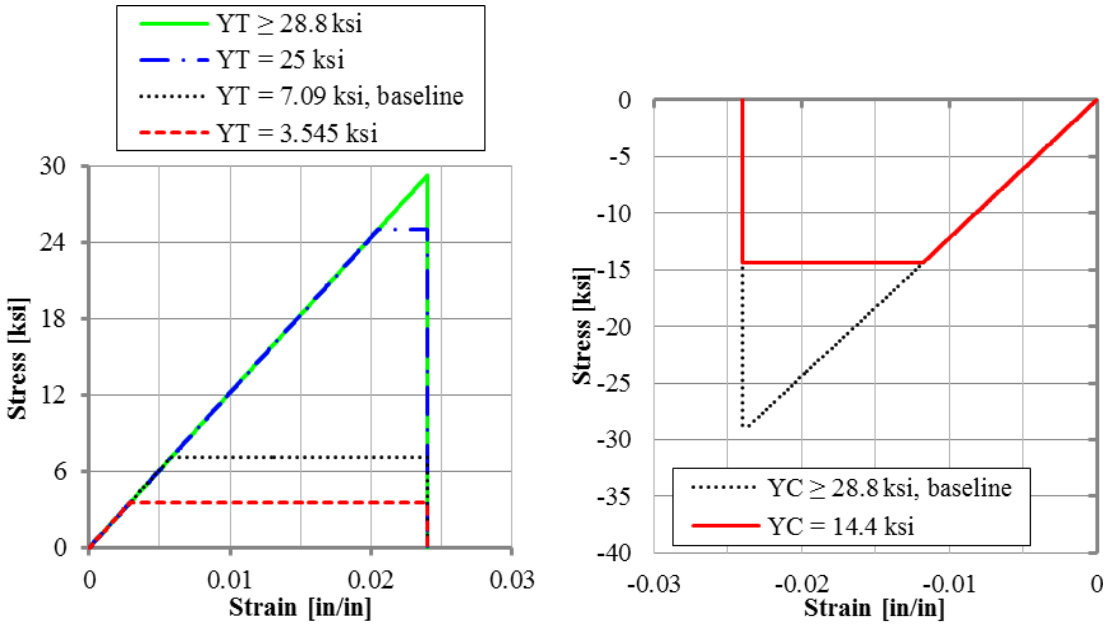

Figure 16. Stress-Strain Curves Resulting From Changing the MAT54 Parameters for Matrix Strength in (a) Tension (YT) and (b) in Compression (YC) in UD $[90]_{12}$ Laminate

Changes in DFAILM had a very strong influence on the matrix single-element model. Lower values underestimated the compressive matrix strength, as shown in figure 17(a), whereas increasing DFAILM so that it was larger than the baseline caused an elongation of the plasticity region in tension and the introduction of a plasticity region in compression. Choosing a zero value for DFAILM caused MAT54 to equate it as numerically infinite; the element continued to strain at a constant ultimate stress level loaded until it was eventually deleted by the violation of the time-step, TFAIL, as shown in figure 17(b).

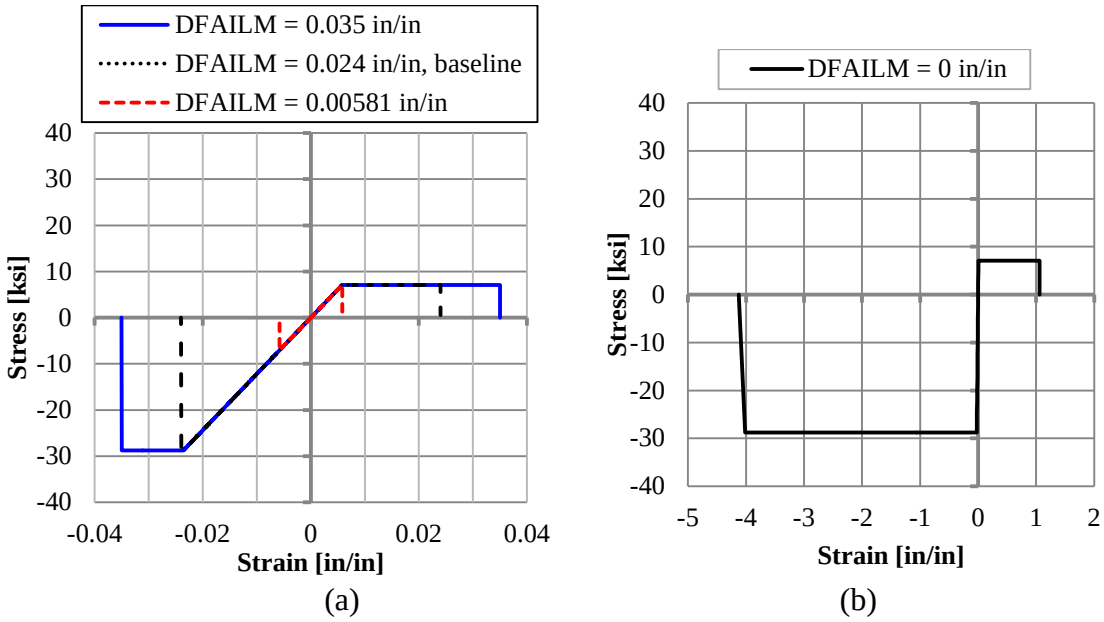

Figure 17. Stress-Strain Results From (a) Changing the Matrix Failure Strain (DFAILM Parameter) and (b) Setting DFAILM to a Zero Value in UD $[90]_{12}$ Laminate

A great consequence of the strong influence of DFAILM was that the choice of defining DFAILM from either equation 15 or 16 had a significant impact on the results. The stress-strain plot in figure 18(a) shows the difference between using equation 15 (DFAILM = 0.00581 in/in), equation 16 (DFAILM = 0.024 in/in), and the expected result, which would be linearly elastic in both tension and compression. The energy outputs from these three cases are plotted in figure 18(b). Table 7 shows the resulting total energy values from this parametric study. The loss of energy from using the tensile DFAILM and gain of energy from using the compressive DFAILM is evidenced in the curves. Therefore, the DFAILM parameter cannot be tailored to give ideal results like DFAILT and DFAILC and will always cause some error. This must be taken into account when using MAT54 to model a composite material system.

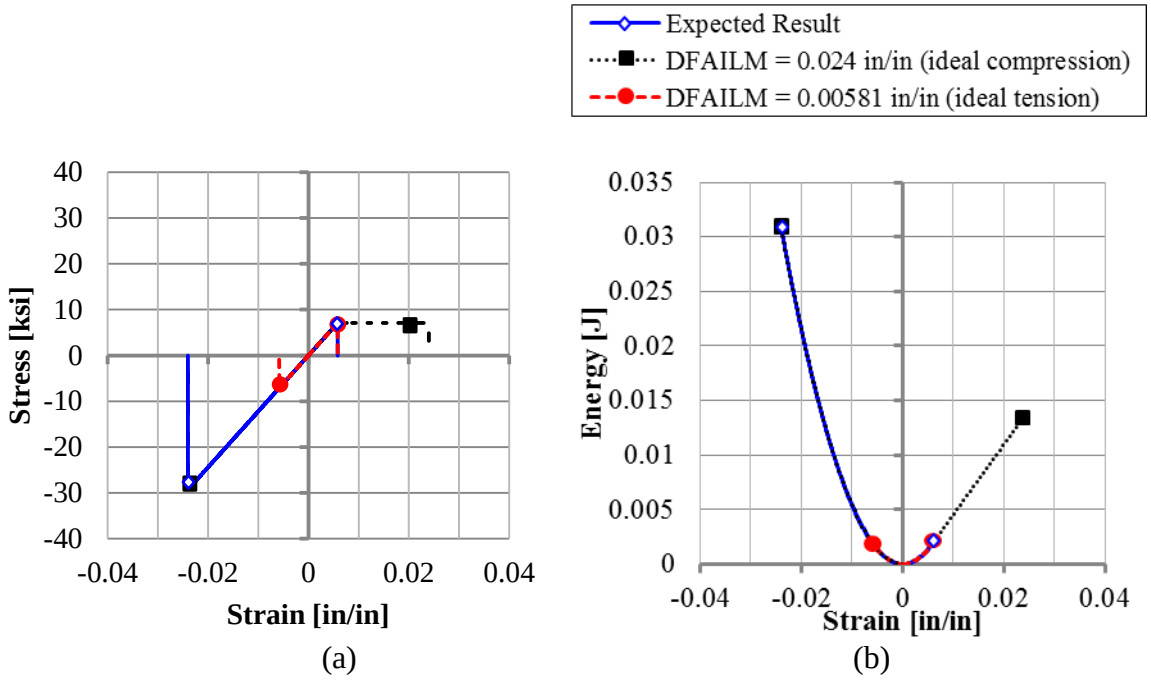

Figure 18. Expected and Simulated (a) Stress-Strain and (b) Energy Curves From Using the Two Possible Baseline DFAILM Values in UD $[90]_{12}$ Laminate

Table 7. Energy Output Values From Ideal DFAILM Simulations

Test Scenario	DFAILM (in/in)	Compression Energy (J)	Tension Energy (J)	Total Energy (J)	Error (%)
Linear Elastic	-	0.0308	0.0018	0.0327	-
Ideal Tension	0.0058	0.0018	0.0018	0.0037	-89
Ideal Compression	0.0240	0.0308	0.0135	0.0443	+36

3.2.5 Discussion of the UD $[0]_{12}$ and $[90]_{12}$ Laminate Results.

These UD single-element studies have shown that, whereas the material strengths are important parameters that affect both the failure and post-failure characteristics, changing the material strengths has less of an effect on the total energy of a simulation than changing the material failure strain parameters that dictate stress reduction and element deletion. This was unexpected because MAT54 uses a stress-based failure criterion and the strength parameters were expected to be highly influential. Instead, the failure strains, which require calculation from known material properties because they are not material properties, largely dictate the results of the UD laminate modeled with MAT54. Considering the failure strain as the critical modeling parameter in MAT54 for simple UD simulations, figure 19 summarizes the failure behavior of a MAT54 element according to the chosen failure strain.

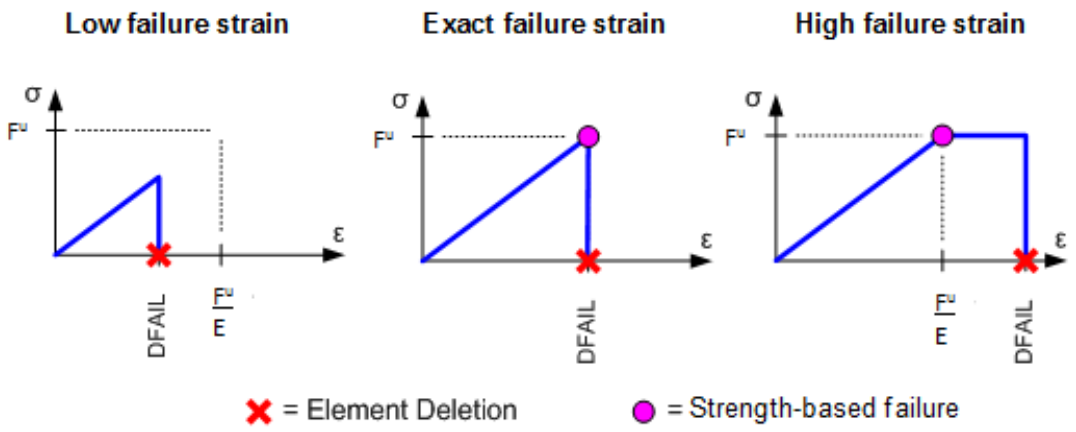

Figure 19. Three Basic Stress-Strain Behaviors Dependent on the MAT54 Failure Strains

For perfectly linear elastic materials, this result is not particularly consequential because an exact failure strain (figure 19) can be defined to avoid plastic behavior or premature element deletion. However, because the maximum strain for matrix straining (DFAILM) defines the failure strain for the matrix in both tension and compression, only one loading case can be satisfied unless the two values are indeed equal, which was not true in this case. Therefore, it is not possible to obtain results for this UD material without error in the transverse direction. In general, the larger of the two DFAILM values is recommended for the sake of simulation stability. If linear elastic behavior is not desired, the failure strains can be modified, but the consequence on the energy should be taken into consideration.

3.3 FABRIC $[(0/90)]_8$ AND UD CROSS-PLY $[0/90]_{3s}$ LAMINATES.

3.3.1 Expected Results.

The properties in table 2 for the fabric material system were used to generate the expected linear stress-strain response of the $[(0/90)]_{8f}$ fabric laminate. The Maximum Stress failure criterion was used to determine the expected behavior of this fiber-dominated laminate, as shown in figure 20. Predicting the response of the $[0/90]_{3s}$ cross-ply laminate required considering individual ply stresses and progressive ply failure. It was expected that the 90-degree plies would fail before the 0-degree plies. Classical laminate theory was used with the MAT54 failure criterion in equations 4–7, and the resulting stress-strain response is also shown in figure 20. The fabric and the cross-ply laminates were very similar in strength and stiffness.

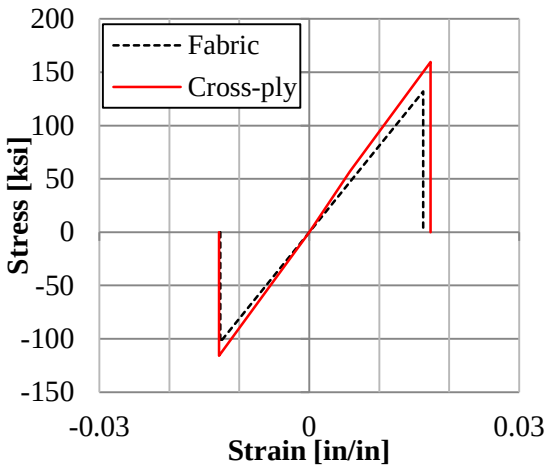

Figure 20. Expected Results of the Fabric and Cross-Ply Laminates as Determined Using the Published Material Property Data

A concern when using MAT54 to simulate a fabric material system is that the transverse failure criteria are meant for predicting the matrix failure of a UD ply in the 90-degree direction. To briefly address this, the failure prediction using the MAT54 failure criterion in the transverse compression loading case (equation 7) was compared against a prediction using the Maximum Stress criterion, which is more appropriate for predicting fiber failure. For this material system and the shear-free loading condition, the difference between the peak stress achieved using Hashin [11] and the peak stress achieved using Maximum Stress criterion was 29 psi. Although this result could imply that using the Hashin criterion for a fabric material is acceptable, it should be considered with caution. These single-element simulations did not include any shear stresses, which play a great role in the Hashin criterion (equation7).

In addition to the calculated expected results, experimental coupon-level tests conducted at the University of Washington provided strength and modulus data for the cross-ply and fabric laminates. Figure 21 shows the results from the $[(0/90)]_{8f}$ fabric and $[0/90]_{3s}$ cross-ply tension and compression coupon tests. The tests of the fabric material system yielded results that were stronger than what is reported in the AGATE material database [15]; however, the modulus was very similar. Experimental results from the cross-ply coupons had excellent matching prior to first ply failure, after which the experimental curve became nonlinear and no longer matched the expected linear results. Otherwise, the measured strength values were very close and the fabric and cross-ply laminates were experimentally shown to behave similarly. This physical similarity was useful when comparing how MAT54 simulates a UD cross-ply laminate (a material system it was designed to simulate) against the simulation of the fabric laminate.

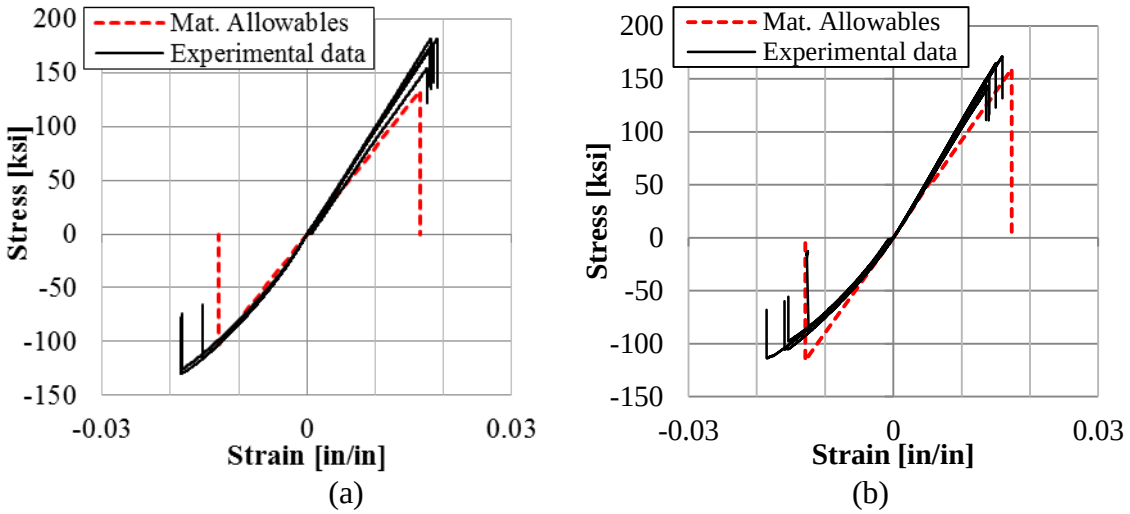

Figure 21. Experimental Stress-Strain Curves From Coupon-Level Tests of (a) $[(0/90)]_8$ Fabric and (b) $[0/90]_{3s}$ Cross-Ply Laminates With Expected Results Based on Material Properties

3.3.2 Baseline Simulation Results.

The baseline fabric single-element simulation produced ply stresses and strains that were equal in each ply because of the uniform $[0]_8$ lay-up. Table 8 shows the peak stress, strain, and energy values for the baseline simulation, for which the expected energy output was determined by calculating the area under the expected linear force-displacement curve. Figure 22 shows the laminate stress-strain curve and output energy, both of which correlated very well with the expected linear elastic stress results as determined by the fabric material properties. The fabric baseline was also simulated using a $[90]_8$ lay-up to test the transverse properties of the material system. A comparison of the longitudinal (0-degree) and transverse (90-degree) stress-strain curves generated by MAT54 (figure 23) demonstrates the similarity of the two fabric directions.

Table 8. Peak Stress, Strain, and Energy Values for the Baseline $[(0/90)]_{8f}$ Fabric Simulation and the Error With the Expected Values

Parameter	Expected	MAT54 Baseline	Error
F_1^{tu}	132 ksi	131.98 ksi	0.0%
F_1^{cu}	-103 ksi	-103.00 ksi	0.0%
ε_1^{tu}	0.0164 in/in	0.01638 in/in	-0.2%
ε_1^{cu}	-0.0130 in/in	-0.01300 in/in	-0.1%
Energy^{tu}	0.09661J	0.09046J	-6.4%
Energy^{cu}	0.05976J	0.05583J	-6.6%

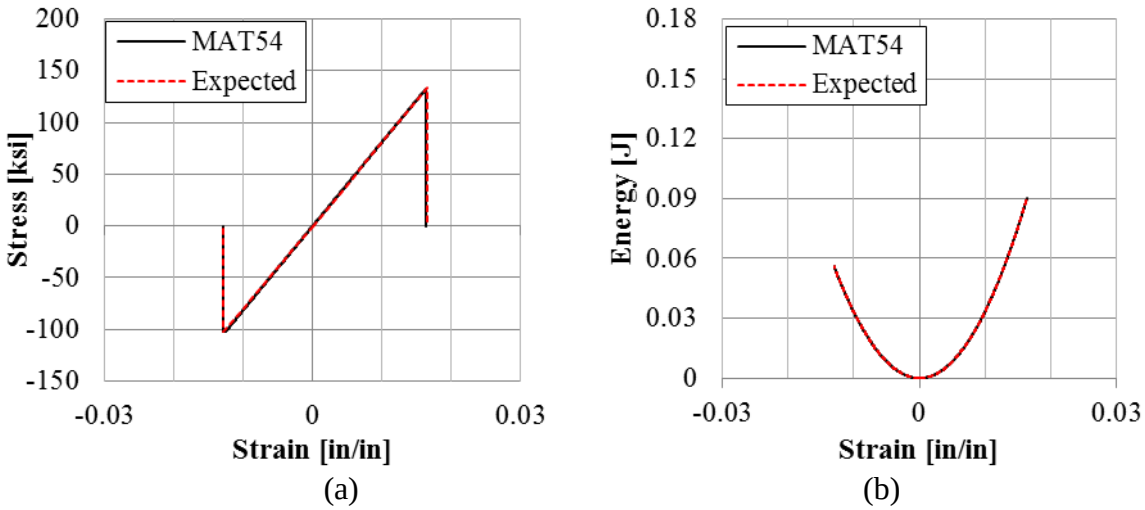

Figure 22. (a) Laminate Stress-Strain and (b) Output Energy Curves for the Baseline Fabric Single-Element Simulation That Exactly Align With Expected Curves

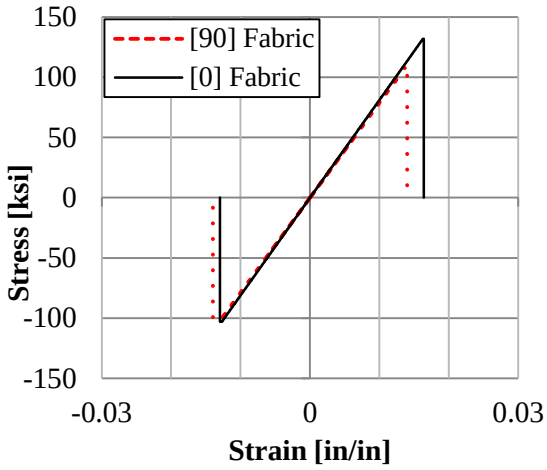

Figure 23. Baseline Fabric Single Element Simulated Using MAT54 in the [0] and [90] Directions

In the elastic region of the stress-strain curve of the baseline cross-ply simulation (figure 24), the simulated curve was identical to the expected results. However, after failure, the simulation continued at a low stress level to plastically strain until the failure strain parameter, DFAILM, was reached. The shape of the simulated curve in figure 24 does not have a meaningful physical interpretation, as the plastic straining was a consequence of the way MAT54 determines element failure from strain parameters. Although MAT54 successfully predicted first ply failure (there was a change of slope when the 90-degree plies failed), ultimate laminate failure was incorrect. To understand how MAT54 generated the cross-ply laminate curve, the 0- and 90-degree ply stresses are shown separately in figure 25. The greater magnitude of the 0-degree ply stresses shows that these plies carried the majority of the stress in the laminate. For a balanced cross-ply laminate, the laminate stress can be determined by averaging the 0- and 90-degree ply stresses. The ply stresses of the 0- and 90-degree plies are superimposed with the laminate stress, shown

in figure 26 in terms of MAT54 user input parameters. From this plot, the influence of each parameter on the cross-ply element can be anticipated; for example, changes in XT are expected to affect the first stress peak in tension of the laminate. This schematic was useful during the parametric studies of the cross-ply element.

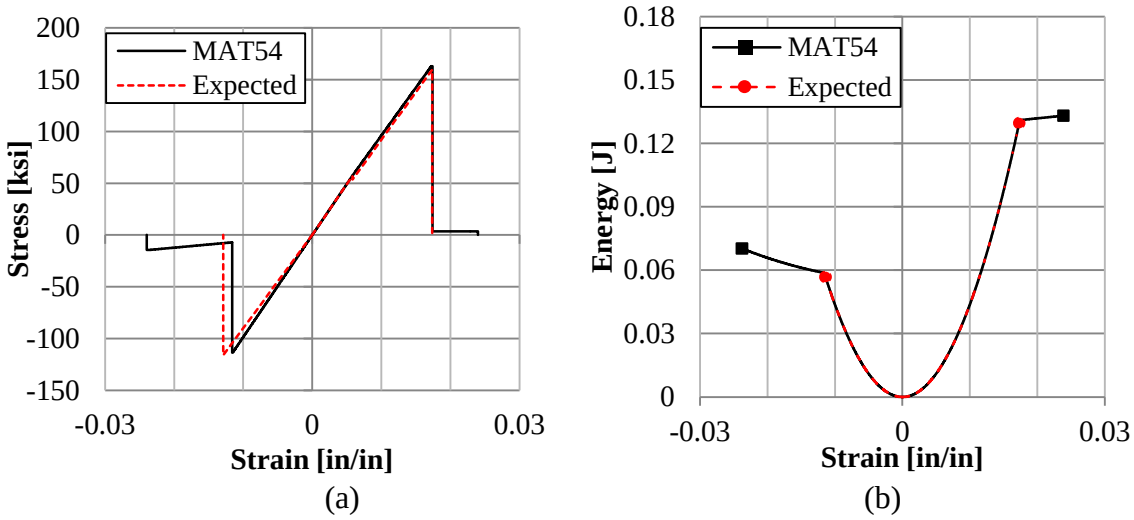

Figure 24. Simulated Baseline Cross-Ply (a) Stress-Strain and (b) Energy Compared With Expected Results

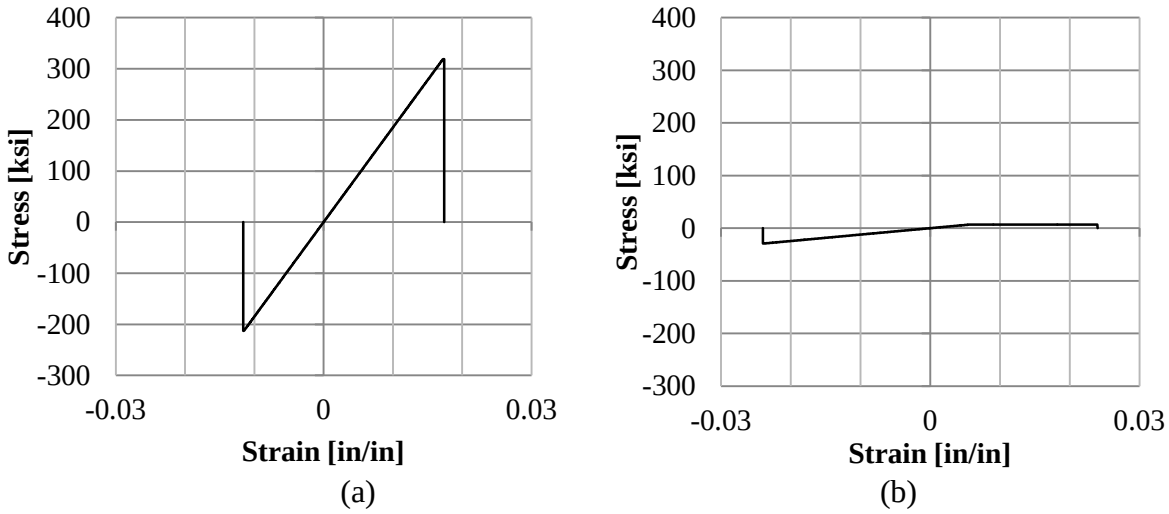

Figure 25. Ply Stresses of the (a) 0-degree and (b) 90-degree Plies in the Cross-Ply Laminate

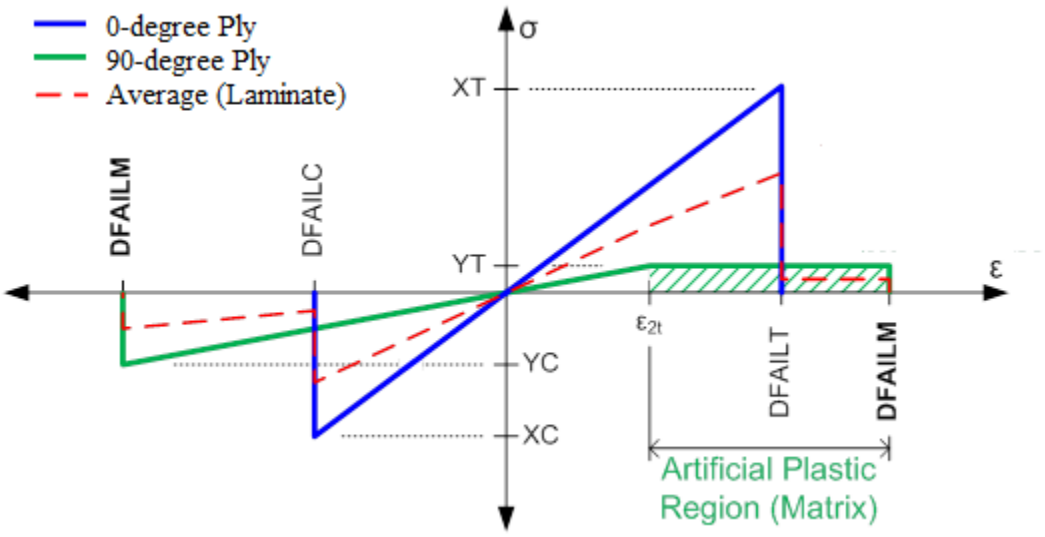

Figure 26. Averaging the Ply Stresses Gives the Laminate Stress, Shown in Terms of LS-DYNA Parameters

Considering the cross-ply laminate stress, the element was not deleted after the 0-degree plies failed. Instead, element deletion occurred only after the 90-degree plies were deleted because of DFAILM. This result once again suggests the importance of the DFAILM parameter in MAT54. The additional stress in the element after failure contributes 7.4% more energy to the simulation than expected. In this case, because the stress level is low during the plastic straining, the additional energy increase is not substantial. Table 9 shows the peak stress, strain, and energy values for the baseline simulation, along with the error of these values against the expected results. The failure strains had the highest error of these parameters because of the plastic straining caused by DFAILM in the simulation; however, the error in energy for the cross-ply laminate is relatively low, unlike the UD laminates, for which the large failure strain errors contributed to significantly large energy errors (see table 4).

Table 9. Peak Stress, Strain, and Energy Values for the Baseline $[0/90]_{3s}$ Cross-Ply Simulation and the Error With the Expected Values

Parameter	Expected	MAT54 Baseline	Error
F_1^{tu}	163.0 ksi	160.0 ksi	-1.8%
F_1^{cu}	-120.9 ksi	-113.5 ksi	-6.1%
ε_1^{tu}	0.0174 in/in	0.024 in/in	38%
ε_1^{cu}	-0.0129 in/in	-0.024 in/in	86%
Energy^{tu}	0.13106J	0.13318J	1.6%
Energy^{cu}	0.05855J	0.07053J	21%

As previously mentioned in section 3.3.1, the experimental stress-strain results from these two laminates were comparable. A comparison of the simulation results from these two laminates also showed similarity (figure 27), except for the error of the failure strains in the UD cross-ply laminate. When choosing between using a [0] lay-up given fabric lamina properties versus a

[0/90] dispersed lay-up with UD lamina properties, the modeler should be aware of these differences.

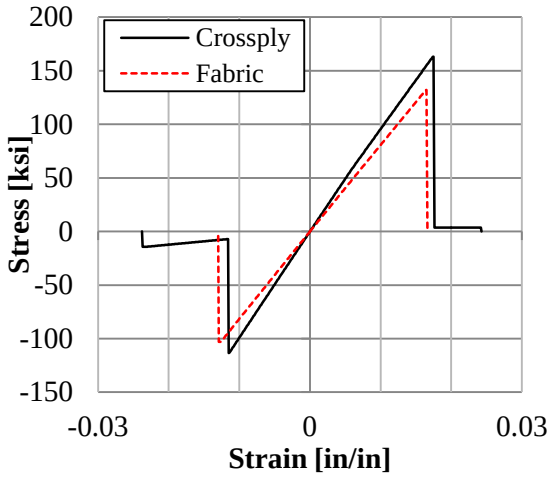

Figure 27. LS-DYNA Simulated Baseline Fabric and Cross-Ply Single-Element Laminates

3.3.3 Results From the Fabric $[(0/90)]_{8f}$ Laminate Parametric Study.

Table 10 shows the test matrix for the study of the influence of MAT54 parameters on the fabric single-element laminate. The parameters that exclusively influenced the transverse direction, such as EB, DFAILM, YC, and YT, were found to have no influence on the fabric simulations in the axial direction. Given the uniform lay-up of the fabric element, it was expected that the trends from the parametric study would be the same as those in the UD single element in section 3.3.2. Simulations of the fabric single element confirmed this expectation.

Table 10. Parametric Test Matrix for the MAT54 Fabric Lay-up, Baseline and Investigated Values

Parameter	Baseline Value	Parametric Value		
XT (ksi)	132	0	75	320
XC (ksi)	103	0	50	200
DFAILT (in/in)	0.0164	0	0.01	0.03
DFAILC (in/in)	-0.0130	0	-0.005	-0.024
DFAILM (in/in)	0.0140	0.005	0.0129	0.024

Changing the fiber modulus, EA, directly affected the stiffness of the stress-strain curve, both in tension and compression (figure 28). Higher EA values caused the element to achieve the strength before the failure strain, and plastic straining followed. Changing the fiber strengths, XT and XC, also changed the peak stress limits (figure 29a). Larger values did not change results because achieving the failure strain deleted the element before it could reach a higher stress. It was expected that the element would fail at a lower strength with respect to smaller strength values. However, in the simulation, using smaller strength values caused plasticity upon

reaching the material strength. This produced energy that was more than 1.5 times higher than what was expected for the low-strength simulation (figure 29b). Although these nonlinear behaviors are not physically correct for this fiber-dominated laminate, the fabric single-element simulation showed the same trends as the UD single element.

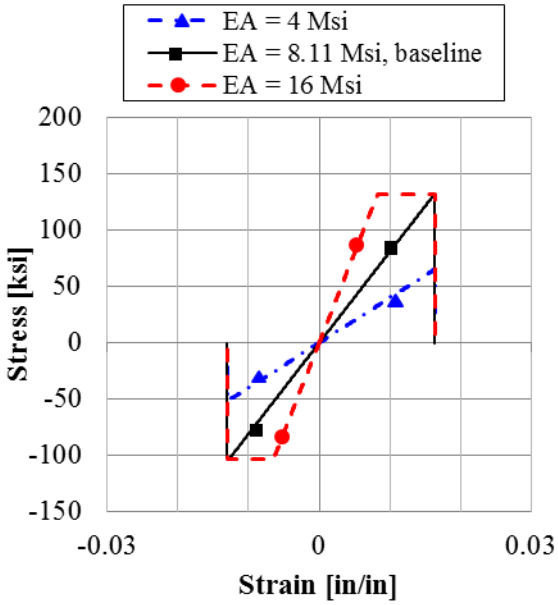

Figure 28. Effect of Changing the Modulus EA on the Fabric Single Element

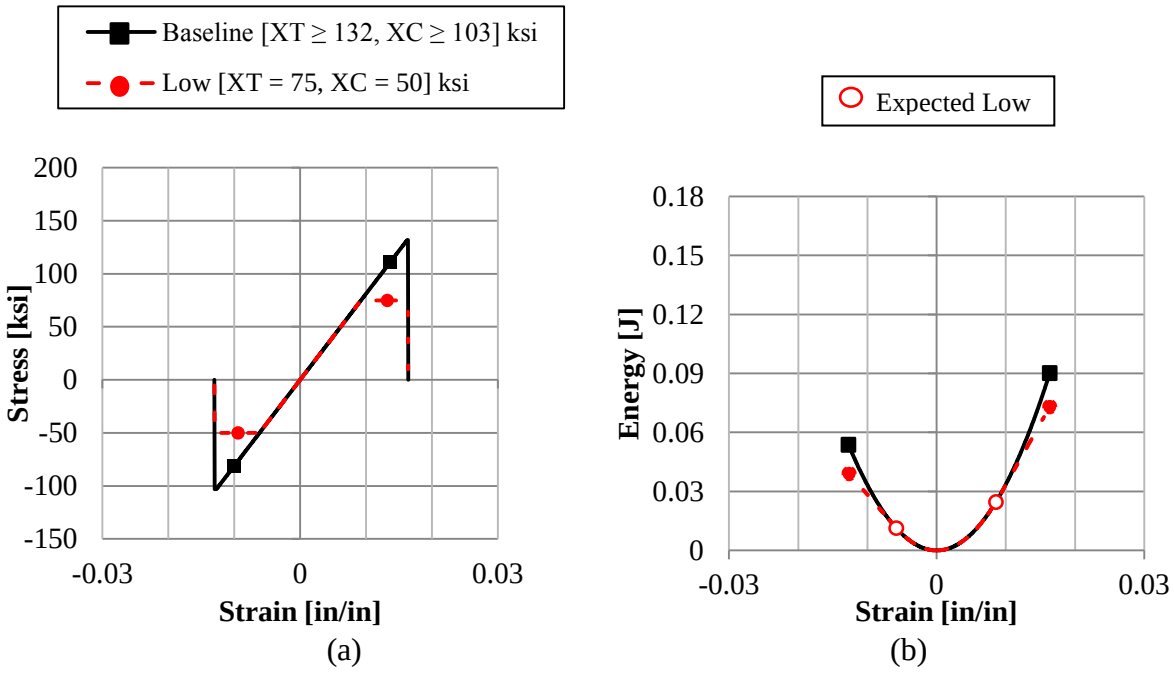

Figure 29. Parametric (a) Stress-Strain and (b) Energy Results From Varying Material Strengths, XT and XC, on the Fabric Single Element

Varying the axial failure strain parameters, DFAILT and DFAILC, also produced the same trends demonstrated by the UD single element. Failure strains larger than the baseline caused plasticity until the new failure strain was reached, whereas decreasing failure strains below the baseline value caused deletion of the element before the material strength was reached (figure 30(a)). These failure strain parameters greatly influenced the energy output by the element, producing values that were 96% above and 91% below the baseline value (figure 30(b)).

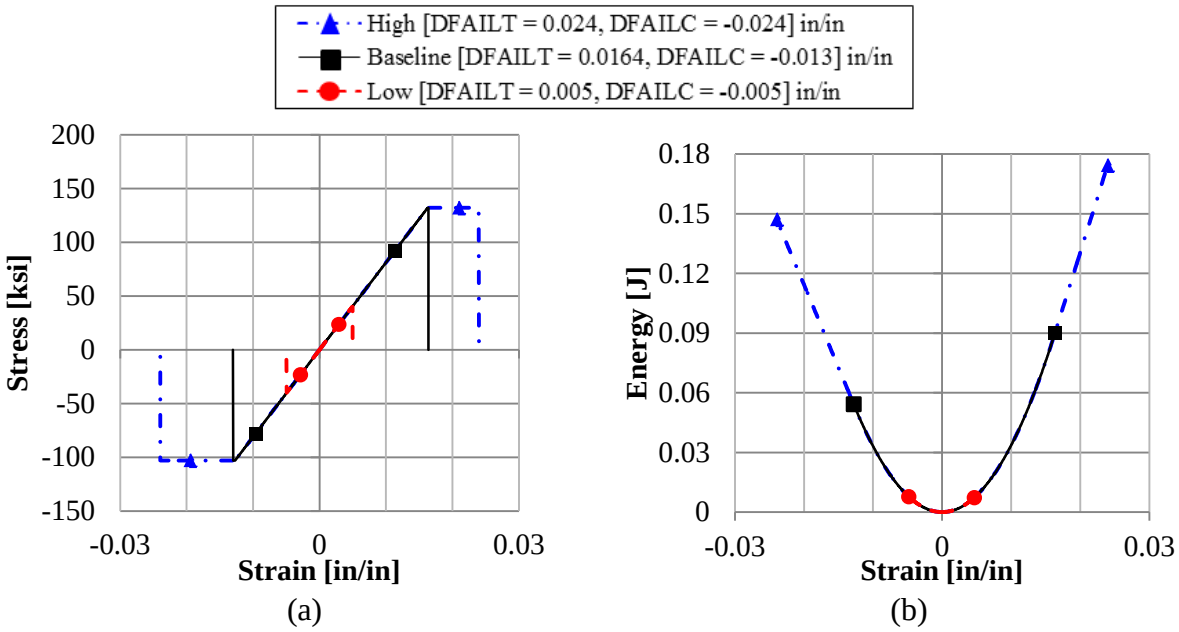

Figure 30. Parametric (a) Stress-Strain and (b) Energy Results From Varying Failure Strains on the Fabric Single Element

Simulations of the fabric element in the transverse direction yielded the same parametric trends as observed for the $[90]_{12}$ UD single element, for which transverse parameters such as EB, YT, YC, and DFAILM had a great influence on the stress-strain and energy results. In essence, the fabric single element, given its uniform $[0]_8$ lay-up as defined in the LS-DYNA *PART_COMPOSITE input card, is the same as the UD $[0]_{12}$ single element in regard to parametric trends. In the case of an axially loaded [0] element, the transverse input parameters have no influence over the simulation results, meaning they could be changed without consequence to the stress-strain behavior of the element. This is an important finding for MAT54 simulations of fabric material systems that have shown the need to increase DFAILM for stability [4].

3.3.4 Results From the UD Cross-Ply $[0/90]_{3s}$ Laminate Parametric Study.

Table 11 shows the test matrix for the study of the influence of MAT54 parameters upon the UD cross-ply single-element laminate. For the cross-ply study, it was important to consider ply stresses as well as laminate stresses to monitor progressive ply failure.

Table 11. Parametric Test Matrix for the MAT54 UD Cross-Ply $[0/90]_{3s}$ Single-Element Laminate, Baseline and Investigated Values

Variable	Baseline Value	Parametric Value				
XT (ksi)	319	2	5	7	160	479
XC (ksi)	213	1	106.5	234.3	----	----
YT (ksi)	7090	1	3	28.8	29.3	----
YC (ksi)	28800	1	14.4	31.68	57.6	----
DFAILT (in/in)	0.0174	0.0087	0.024	0.025	----	----
DFAILC (in/in)	-0.0116	-0.0058	-0.0087	-0.01276	-0.0174	-0.024
DFAILM (in/in)	0.0240	0.0058	0.0087	0.0174	0.0264	----

Changing the fiber modulus parameter, EA, had a great influence on the stiffness of the cross-ply single element (figure 31(a)) because the majority of the stress in this laminate is carried in the 0-degree plies. Following the 0-degree ply failure, the simulation with varying EA values does not change from the baseline. The 0- and 90-degree ply stresses (figures 31(b and c)) show that EA greatly affected the 0-degree plies, but had no effect on the 90-degree plies, as expected. However, changing the matrix modulus, EB, changed the stiffness of the 90-degree plies only, which had little effect on the stiffness of the entire element and none on the 0-degree plies (figure 32).

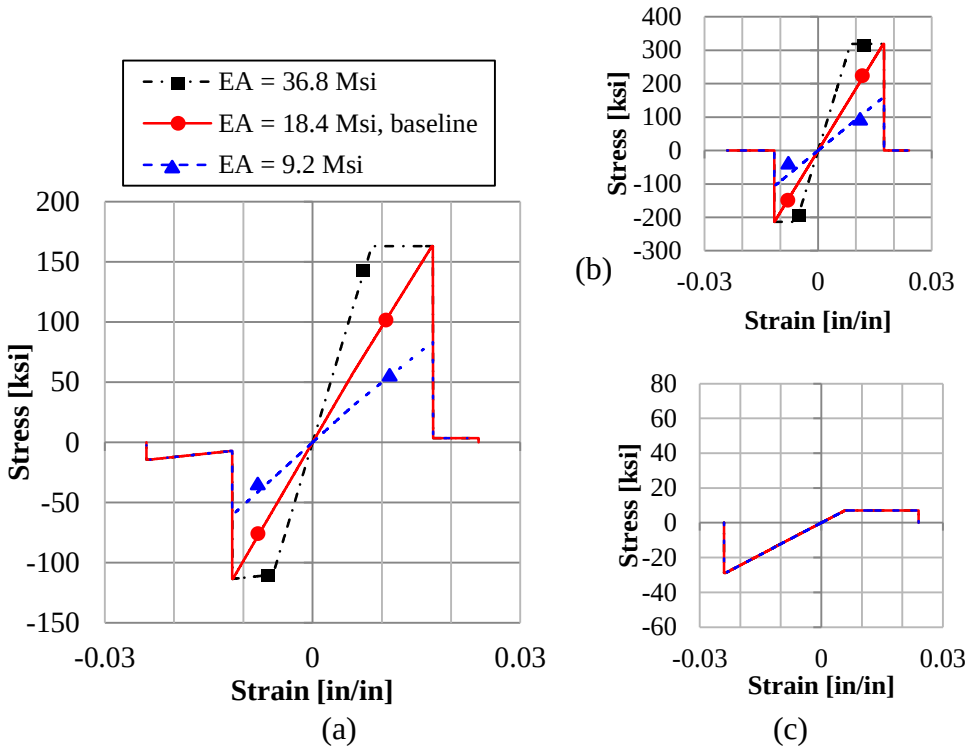

Figure 31. Stress-Strain Results From Changing EA on the (a) Whole Element, (b) 0-Degree Plies, and (c) 90-Degree Plies in the UD Cross-Ply $[0/90]_{3s}$ Single-Element Laminate

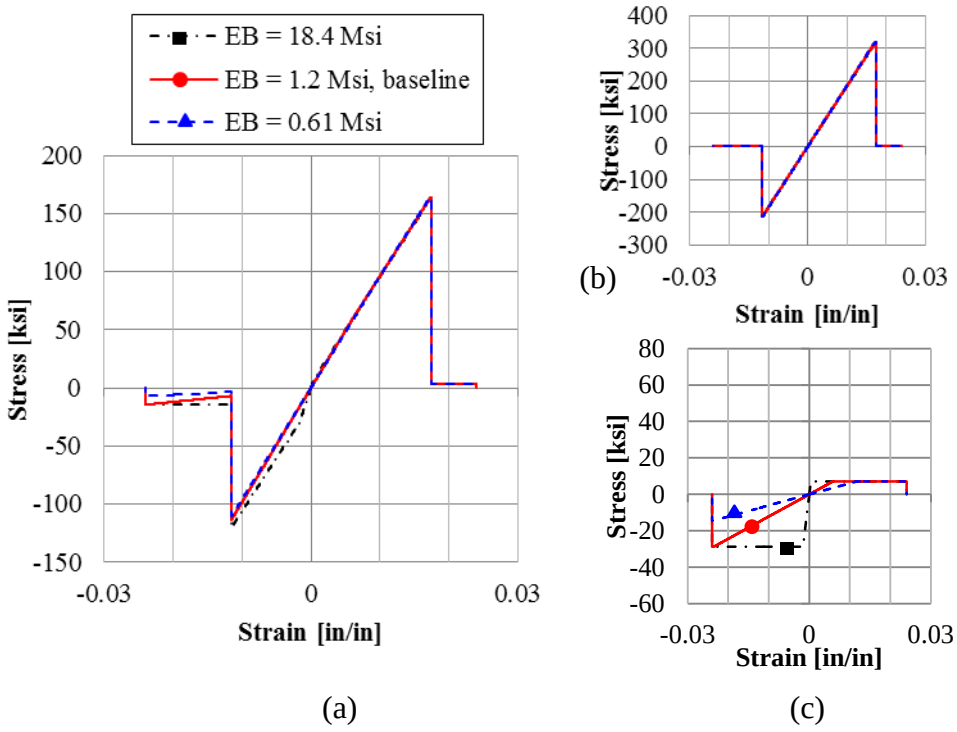

Figure 32. Effect of Changing EB on the Cross-Ply Single-Element (a) Laminate, (b) 0-Degree Plies, and (c) 90-Degree Plies in UD Cross-Ply $[0/90]_{3s}$ Single-Element Laminate

Changing the fiber strength parameters only affected the stress in the loading direction of the 0-degree plies. Changing XT affected the peak stress limit of the 0-degree plies in tension, whereas changing XC affected the peak stress limit of these plies in compression. Varying XT and XC greatly changed the total laminate response (figure 33), in which larger strength values did not change results, but smaller values caused plasticity.

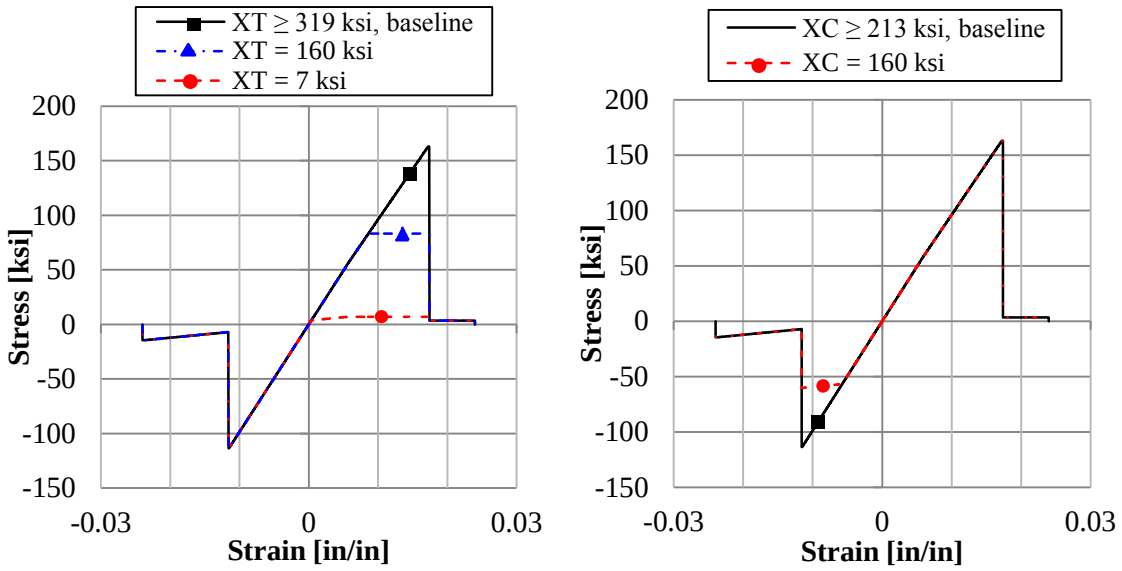

Figure 33. Effect of (a) XT and (b) XC on the Stress-Strain Curve of UD Cross-Ply $[0/90]_{3s}$ Single-Element Laminate

The energy losses associated with reduced-strength values (figure 34) were not as severe as would be physically expected because the plasticity provided additional energy that would have otherwise been lost.

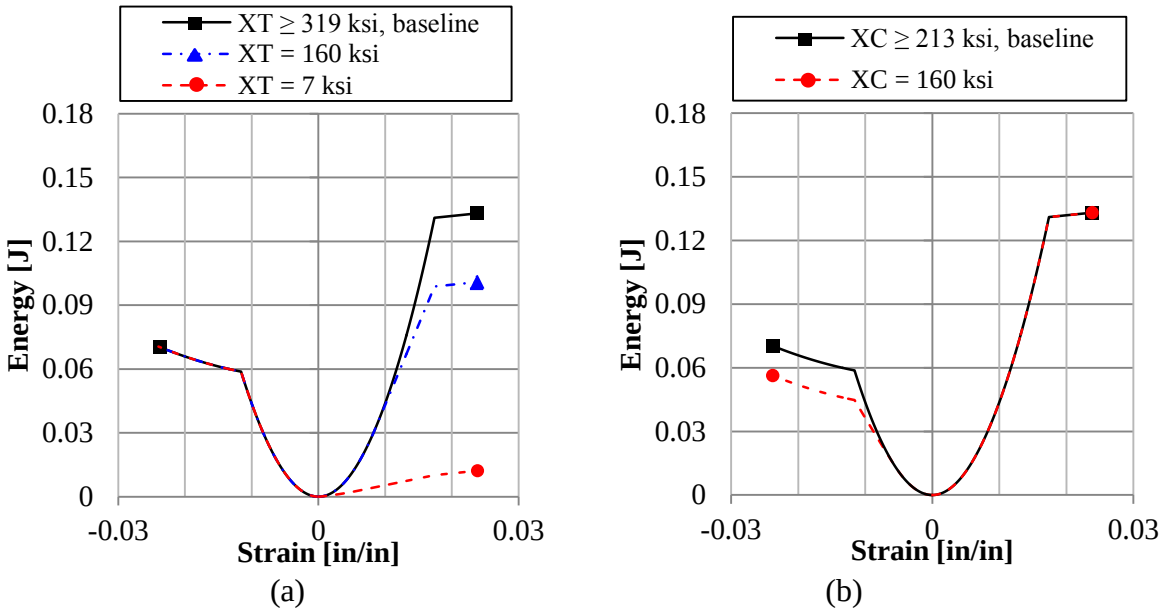

Figure 34. Effect of (a) XT and (b) XC on the Laminate Output Energy of the UD Cross-Ply $[0/90]_{3s}$ Single-Element Laminate

The matrix strength parameters, YT and YC, have a similar effect on the 90-degree plies as the XT and XC parameters had on the 0-degree plies. However, the effect on the laminate stress response is inconsequential because the 90-degree plies carry little stress in the laminate. Changing YT had only a very slight effect on the laminate stress in tension (figure 35(a)). The only noticeable change is in regard to the stress in the 90-degree plies, as shown in figure 35(b).

Figure 35(b) shows that higher values of YT increased the stress value at which plasticity occurs and lower values decreased this stress limit. The overall energy increase in the laminate was only 7% when YT was increased more than four times above the baseline value. In compression, changing only YC affected the 90-degree plies as well, whereas the laminate stress response was not significantly altered (figure 36). Halving YC resulted in an energy decrease in the laminate of only 6% below the baseline. For this material system, transverse strength values are not critical MAT54 parameters in a laminate that has fiber-dominance in the two principle directions.

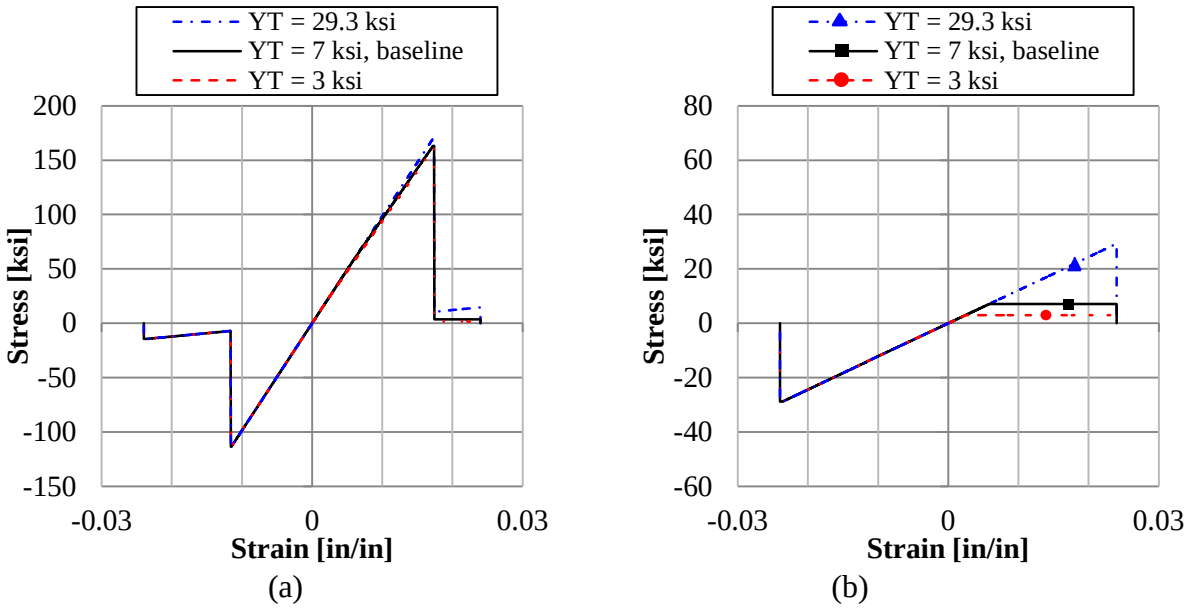

Figure 35. Effect of YT on the UD Cross-Ply $[0/90]_{3s}$ Single-Element Laminate on the (a) Laminate Stress and (b) 90-Degree Ply Stresses

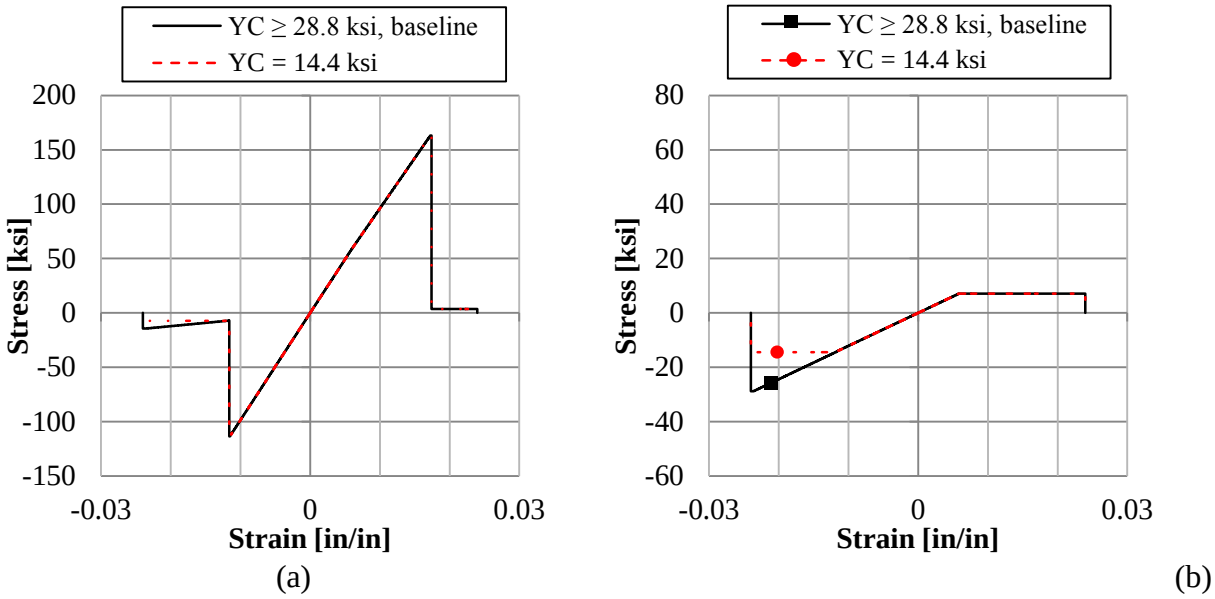

Figure 36. Effect of YC on the UD Cross-Ply $[0/90]_{3s}$ Single-Element Laminate on the (a) Laminate Stress and (b) 90-Degree Ply Stresses

Changes in the fiber failure strains, DFAILT in tension and DFAILC in compression, significantly changed the cross-ply laminate stress results (figure 37) because these parameters controlled the deletion of the 0-degree plies. Smaller values reduced the peak stress magnitude because the 0-degree plies would be deleted prior to reaching the material strength. Larger values created plasticity at the peak stress value until 0-degree ply deletion. These variations

greatly impacted the energy of the simulations, as shown in figure 38. In the case of the DFAILT value 44% greater than the baseline (DFAILT = 0.025 in/in), the energy increases 83% above the baseline value.

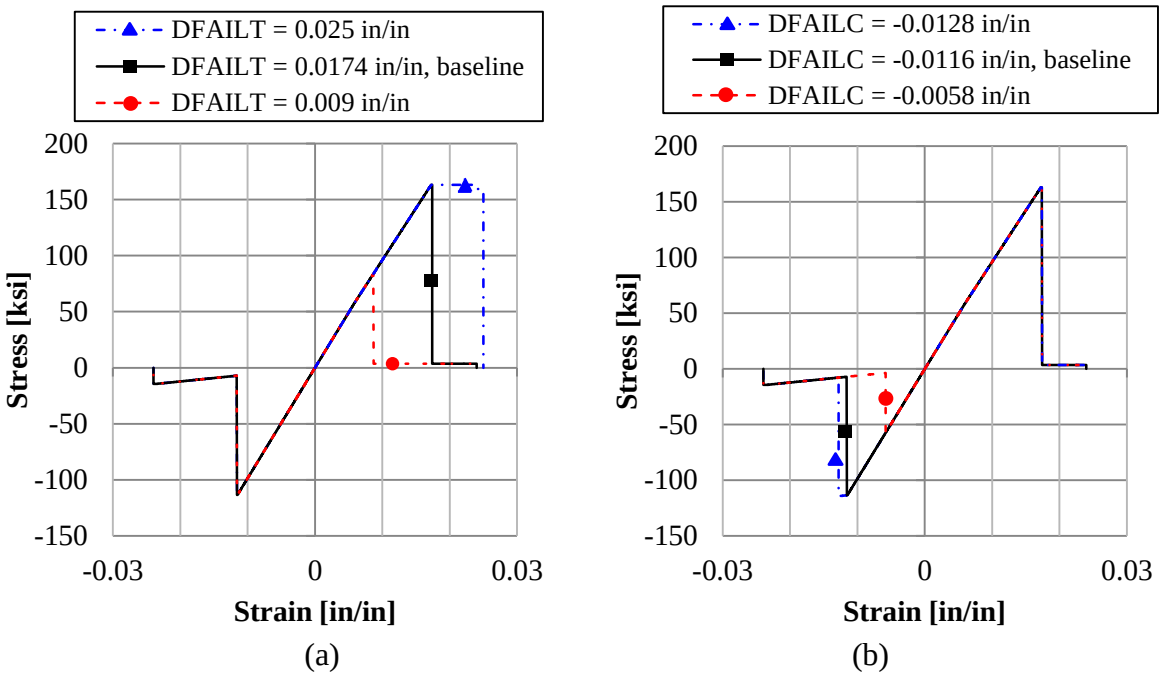

Figure 37. Effect of (a) DFAILT and (b) DFAILC on the Stress-Strain Curve of the UD Cross-Ply $[0/90]_{3s}$ Single-Element Laminate

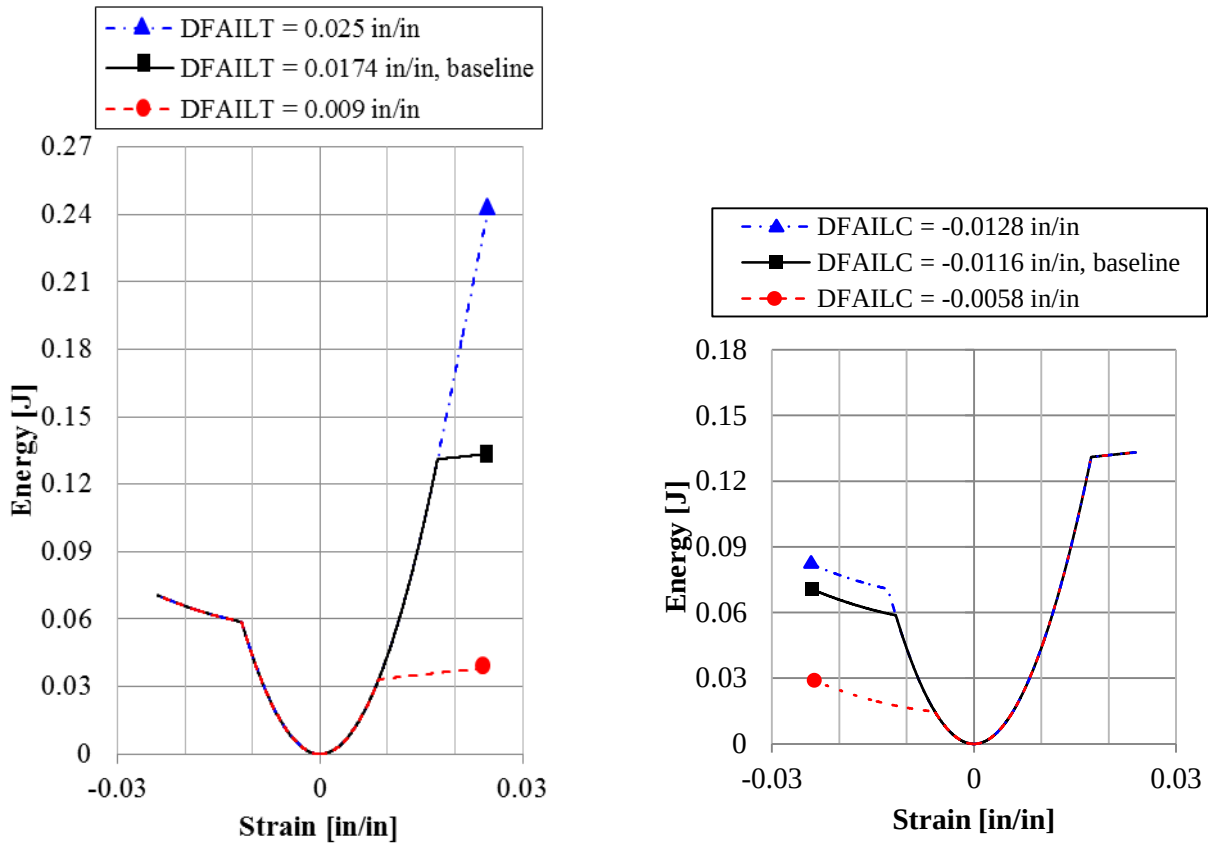

(a) (b)

Figure 38. Effect of (a) DFAILT and (b) DFAILC on the Energy Output of the UD Cross-Ply $[0/90]_{3s}$ Single-Element Laminate

The deletion of the 90-degree plies depended on the matrix failure strain DFAILM. Because the element was deleted only after all of the plies had been deleted, DFAILM also directly affected element deletion. Lowering DFAILM lowered the strain to failure of the element and shortened the plasticity region in tension (figure 39a), whereas raising DFAILM had the opposite effect. Because the 90-degree plies had so little influence on the overall laminate response, changes in DFAILM were relatively inconsequential to the element stress response. This is important because the transverse material response can be linearly elastic only in one loading case, depending on the determination of DFAILM in equations 15 or 16. This limits the MAT54 user to defining the 90-degree failure strain in either tension or compressions—never both. Although the effect on the stress of changing DFAILM was small, the resulting difference in energy was slightly more significant. Considering the two perfectly linear elastic values, DFAILM = 0.024 in/in in compression and DFAILM = 0.0058 in/in in tension, figure 39(b) shows the -5.3% in tension and -21% in compression energy loss associated with using the smaller DFAILM value.

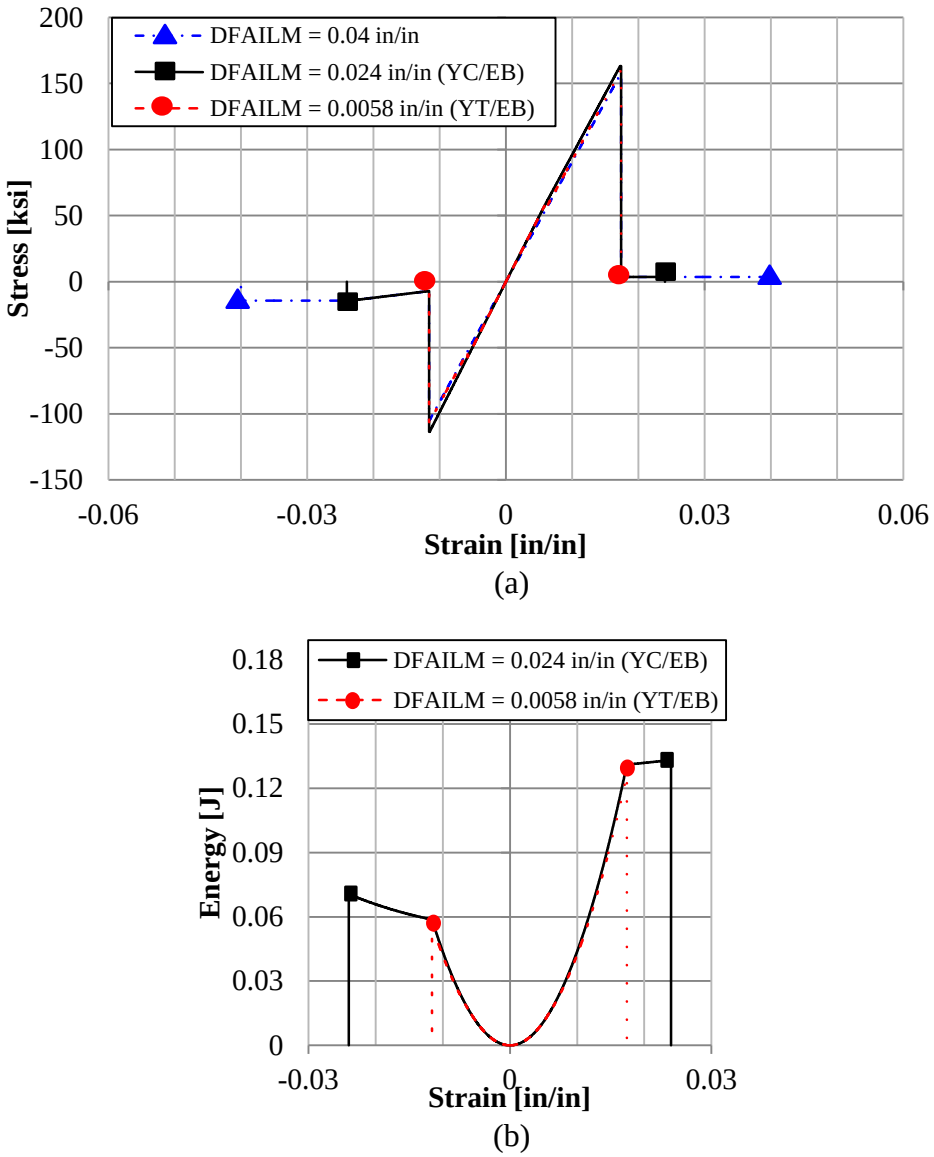

Figure 39. Effect of Changing DFAILM in the UD Cross-Ply $[0/90]_{3s}$ Single-Element Laminate on the (a) Laminate Stress and (b) Energy Output

4. CONCLUSIONS.

This report summarized the results of an investigation into the LS-DYNA composite material model MAT54 using single elements to characterize the model. First, a parametric study of single elements using MAT54 to simulate composite unidirectional (UD) laminates with $[0]_{12}$ and $[90]_{12}$ lay-ups revealed the failure mechanisms, post-failure behavior, and critical parameters for this material model. In MAT54, plies progressively fail based on a stress-based failure criterion; however, a failed ply will remain in its ultimate stressed state after failure. A failed element will continue to strain until the user-defined failure strain is reached and, at that point, only the stress is set to zero and the element is deleted. Although the material strengths are important parameters that affect both the failure and post-failure characteristics, changing the

material strengths has less of an effect on the total energy of a simulation than changing the material failure strain parameters that dictate stress reduction and element deletion. This result was not expected because the MAT54 material model uses a stress-based failure criterion and the strength parameters were expected to be highly influential. Instead, the failure strains, which require calculation from known material properties because they are not material properties, largely dictate the results of the UD laminate modeled with MAT54.

For perfectly linear elastic materials, this result is not particularly consequential because an exact failure strain can be defined to avoid plastic behavior or premature element deletion. However, because the maximum strain for matrix straining (DFAILM) defines the failure strain for the matrix in both tension and compression, only one loading case can be satisfied unless the two values are indeed equal, which they were not in this case. Therefore, it is not possible to obtain results for this UD material without error in the transverse direction. In general, the larger of the two DFAILM values is recommended for the sake of simulation stability. If linear elastic behavior is not desired, the failure strains can be modified, but the consequence on the energy should be taken into consideration.

Secondly, MAT54 was shown to be capable of simulating basic behaviors of a plain-weave fabric material system and a comparable UD cross-ply laminate. Experimentally, these two laminates were shown to be similar because they were made from the same carbon fiber and epoxy constituents. The baseline simulations for these laminates were also similar, except for a noticeable error in the strain-to-failure values of the cross-ply laminate, which were overestimated because of the large strain necessary in the model to remove the 90-degree UD plies. As a result of this error, the shape of the stress-strain curve for the cross-ply laminate was not physically accurate.

Addressed was the concern regarding predicting the failure of a fiber-dominated fabric material in the transverse direction using criteria meant for matrix materials. Opting to use the Maximum Stress failure criterion in place of Hashin [11] had minimal effects on the failure stress; however, the shear-free single-element model is likely to have oversimplified the problem. It is expected that, given more complex loading, the differences between using Hashin and Maximum Stress for the fabric material system could be significant.

The sensitivity of the fabric single element toward the MAT54 parameters was dependent on the direction of the applied load relative to the local material axes. Axial loads were sensitive only to fiber input parameters, whereas transverse loads were sensitive only to matrix input parameters. However, the UD cross-ply element was primarily sensitive to fiber properties, whereas matrix properties had only a very slight significance. For this laminate, loading direction was inconsequential because the number of 0- and 90-degree plies in the lay-up was exactly the same axially and transversely. The cross-ply single element was also strongly influenced by the fiber failure strain parameters, but significantly less so by the matrix failure strain, DFAILM, given that the 90-degree plies contributed little to carrying load within the laminate.

5. REFERENCES.

1. Composite Materials Handbook-17 (CMH-17) Volume 3, Chapter 16, Rev. G.

2. Soden, P.D., Kaddour, A.S., and Hinton, M.J., "Recommendations for Designers and Researchers Resulting From the World-Wide Failure Exercise," *Composite Science and Technology*, Vol. 64, 2004, pp. 589–604.

3. Gabrys, J., Schatz, J., Carney, K., Melis, M., Fasanella, E., and Lyle, K., "The Use of LS-DYNA in the Columbia Accident Investigation and Return to Flight Activities," *Proceedings of the 8th International LS-DYNA User's Conference*, Detroit, Michigan, May 2004.

4. Feraboli, P., Deleo, F., Wade, B., et al, "Predictive Modeling of an Energy-Absorbing Sandwich Structural Concept Using the Building Block Approach," *Composites: Part A*, Vol. 41, 2010, pp. 774–786.

5. Ensan, M.N., Zimcik, D.G., Lahoubi, M., and Andrieu, D., "Soft Body Impact Simulation on Composite Structures," *Transactions of the CSME*, Vol. 32, 2008, pp. 283–296.

6. Hörmann, M. and Wacker, M., "Simulation of the Crash Performance of Crash Boxes Based on Advanced Thermoplastic Composite," *Proceedings of the 5th European LS-DYNA User's Conference*, Birmingham, United Kingdom, 2005.

7. Fasanella, E.L. and Jackson, K.E., "Best Practices for Crash Modeling Simulation," NASA TM-2002-211944, ARL-TR-2849, October 2002.

8. Livermore Software Technology Corporation, *LS-DYNA Keyword User's Manual Version 971*, May 2007.

9. Chang, F.K. and Chang, K.Y., "A Progressive Damage Model for Laminated Composites Containing Stress Concentration," *Journal of Composite Materials*, Vol. 21, 1987, pp. 283–296.

10. Hahn, H.T. and Tsai, S.W., "Nonlinear Elastic Behavior of Unidirectional Composite Laminate," *Journal of Composite Materials*, Vol. 7, 1973, pp. 102–110.

11. Hashin Z., "Failure Criteria for Unidirectional Fiber Composites," *Journal of Applied Mechanics*, Vol. 47, 1980, pp. 329–334.

12. Tsai, S.W. and Wu, E.M., "A General Theory of Strength for Anisotropic Materials," *Journal of Composite Materials*, Vol. 5, 1971, pp. 58–80.

13. Feraboli, P., Wade, B., Deleo, F., Rassaian, M., Higgins, M., and Byar, A., "LS-DYNA MAT54 Modeling of the Axial Crushing of a Composite Tape Sinusoidal Specimen," *Composites: Part A*, Vol. 42, 2011, pp. 1809–1825.

14. Tomblin, J., Sherraden, J., Seneviratne, W., and Raju, K.S., "A-Basis and B-Basis Design Allowables for Epoxy-Based Prepreg: Toray T700GC-12k-31E/#2510 Unidirectional Tape," NASA AGATE Program, AGATE-WP3.3-033051-135, October 2002.

15. Tomblin, J., Sherraden, J., Seneviratne, W., and Raju, K.S., “A-Basis and B-Basis Design Allowables for Epoxy-Based Prepreg: Toray T700SC-12k-50C/#2510 Plain-Weave Fabric,” NASA AGATE Program, AGATE-WP3.3-033051-131, September 2002.

16. Courant R, Friedrichs K, Lewy H. Über die partiellen Differentialgleichungen der mathematischen Physik, *Mathematische Annelen*, 100 (1928) 32–74.

APPENDIX A—LS-DYNA THEORY MANUAL FOR MATERIAL MODEL MAT54

The MAT54 material model uses the MAT22 stress-strain equations in the elastic region; therefore, the appropriate portion from the LS-DYNA Theory Manual [A-1] for MAT22 is presented here in addition to the entire section of the LS-DYNA Theory Manual for the MAT54 material model.

MAT22: Chang-Chang Composite Failure Model
In plane stress, the strain is given in terms of the stress as:

$$\varepsilon_1 = \frac{1}{E_1}(\sigma_1 - \nu_{12}\sigma_2) \tag{A-1}$$

$$\varepsilon_2 = \frac{1}{E_2}(\sigma_2 - \nu_{21}\sigma_1) \tag{A-2}$$

$$2\varepsilon_{12} = \frac{1}{G_{12}}\tau_{12} + \alpha{\tau_{12}}^3 \tag{A-3}$$

Equation A-3 defines the nonlinear shear stress parameter α.

MAT54 and MAT55: Enhanced Composite Damage Model
These models are very close in their formulations. MAT54 uses Chang matrix failure criterion (as MAT22) and MAT55 uses the Tsai-Wu criterion for matrix failure.

Arbitrary orthotropic materials (e.g., unidirectional layers in composite shell structures) can be defined. Optionally, various types of failure can be specified following either the suggestions of Chang and Chang [A-2] or Tsai and Wu [A-3]. In addition, special measures are taken for failure under compression [A-4]. This model is valid only for thin-shell elements.

The Chang/Chang criteria are given as follows:

for the tensile fiber mode:

$$\sigma_{aa} > 0 \quad then \quad e_f^2 = \left(\frac{\sigma_{aa}}{X_t}\right)^2 + \beta\left(\frac{\sigma_{ab}}{S_c}\right) - 1 \begin{cases} \geq 0 \; failed \\ < 0 \; elastic \end{cases} \tag{A-4}$$

On failure: $E_1 = E_2 = G_{12} = \nu_{12} = \nu_{21} = 0$

for the compressive fiber mode:

$$\sigma_{aa} < 0 \quad then \quad e_c^2 = \left(\frac{\sigma_{aa}}{X_{tc}}\right)^2 - 1 \begin{cases} \geq 0 \; failed \\ < 0 \; elastic \end{cases} \tag{A-5}$$

On failure: $E_1 = \nu_{12} = \nu_{21} = 0$

for the tensile matrix mode:

$$\sigma_{bb} > 0 \quad then \quad e_m^2 = \left(\frac{\sigma_{bb}}{Y_t}\right)^2 + \left(\frac{\sigma_{ab}}{S_c}\right)^2 - 1 \begin{cases} \geq 0 \; failed \\ < 0 \; elastic \end{cases} \tag{A-6}$$

On failure: $E_2 = \nu_{21} = G_{12} = 0$

and for the compressive matrix mode:

$$\sigma_{bb} < 0 \quad then \quad e_d^2 = \left(\frac{\sigma_{bb}}{2S_c}\right)^2 + \left[\left(\frac{Y_c}{2S_c}\right)^2 - 1\right]\frac{\sigma_{bb}}{Y_c} + \left(\frac{\sigma_{ab}}{S_c}\right)^2 - 1 \begin{cases} \geq 0 \; failed \\ < 0 \; elastic \end{cases} \tag{A-7}$$

On failure: $E_2 = \nu_{21} = \nu_{12} = 0 = G_{12} = 0$
$X_c = 2Y_c$ for 50% fiber volume

For $\beta = 1$, the result is the original Hashin [A-5] in the tensile fiber mode.

For $\beta = 0$, the result is the Maximum Stress criterion, which is found to compare better to experiments.

Failure can occur in any of four ways:

1. If DFAILT is zero, failure occurs if the Chang/Chang failure criterion is satisfied in the tensile fiber mode.

2. If DFAILT is greater than zero, failure occurs if the tensile fiber strain is greater than DFAILT or less than DFAILC.

3. If EFS is greater than zero, failure occurs if the effective strain is greater than EFS.

4. If TFAIL is greater than zero, failure occurs according to the element time step as described in the definition of TFAIL.

When failure has occurred in all of the composite layers (through-thickness integration points), the element is deleted. Elements that share nodes with the deleted element become crashfront elements and can have their strengths reduced by using the SOFT parameter with TFAIL greater than zero.

Information about the status in each layer (integration point) and element can be plotted using additional integration point variables. The number of additional integration point variables for shells written to the LS-DYNA database is input by the *DATABASE_BINARY definition as variable NEIPS. For MAT54 and MAT55, these additional variables are tabulated below (*i* = shell integration point):

History Variable	Description	Value	LS-PREPOST History Variable
ef(i)	tensile fiber mode	1 – *elastic* 0 – *failed*	1
ec(i)	compressive fiber mode		2
em(i)	tensile matrix mode		3
ed(i)	compressive matrix mode		4
efail	max[ef(ip)]		5
dam	damage parameter	-1 – *element intact* 10^{-8} – *element in crashfront* +1 – *element failed*	6

The following components, defined by the sum of failure indicators over all through-thickness integration points, are stored as element component 7 instead of the effective plastic strain:

Description	Integration point
$\frac{1}{nip}\sum_{i=1}^{nip} ef(i)$	1
$\frac{1}{nip}\sum_{i=1}^{nip} ec(i)$	2
$\frac{1}{nip}\sum_{i=1}^{nip} em(i)$	3

REFERENCES.

A-1. Livermore Software Technology Corporation, *LS-DYNA Theory Manual*, Sections 19.22 and 19.54, March 2006.

A-2. Chang, F.K. and Chang, K.Y., "Post-Failure Analysis of Bolted Composite Joints in Tension or Shear-Out Mode Failure," *Journal of Composite Materials*, Vol. 21, 1987, pp. 809–833.

A-3. Tsai, S.W. and Wu, E.M., "A General Theory of Strength for Anisotropic Materials," *Journal of Composite Materials*, Vol. 5, 1971, pp. 58–80.

A-4. Matzenmiller, A., and Schweizerhof, K., "Crashworthiness Simulations of Composite Structures—A First Step With Explicit Time Integration," in *Nonlinear Computational Mechanics—A State of the Art*, Wriggers, P.W., et al., ed., Springer-Verlag, Berlin, Germany, 1991, pp. 642–670.

A-5. Hashin, Z., "Failure Criteria for Unidirectional Fiber Composites," *Journal of Applied Mechanics*, Vol. 47, 1980, pp. 329–335.

APPENDIX B—MAT54 INPUT PARAMETER SUGGESTED VALUES

Parameter	Definition	Suggested Value
MID	Material identification number	Any arbitrary integer
RO	Mass per unit volume*	ρ from material properties*
EA	Young's modulus in longitudinal direction	E_1, from material properties
EB	Young's modulus in transverse direction	E_2, from material properties
PRBA	Minor Poisson's ratio, $\nu_{ba} = \nu_{21}$	Calculated using ν_{12} , E_1, and E_2
PRCA	Minor Poisson's ratio, $\nu_{ca} = \nu_{31}$	Not used
PRCB	Minor Poisson's ratio, $\nu_{cb} = \nu_{32}$	Not used
GAB	Shear modulus, G_{ab}	G_{12}, from material properties
GBC	Shear modulus, G_{bc}	Assumed equal to G_{ab}
GCA	Shear modulus, G_{ca}	Assumed equal to G_{ab}
KF	Bulk modulus of material	Not used
AOPT	Material axes option parameter	AOPT = 0
A1 A2 A3 D1 D2 D3	Vector components to define material axes for aopt = 2	Not used
MANGLE	Material angle in degrees used when aopt = 3	Not used
V1 V2 V3	Vector components to define the material axes for aopt = 3	Not used
DFAILT	Max strain for fiber tension	DFAILT = (F_1^{tu} / E_1) [DFAILT > 0]
DFAILC	Max strain for fiber compression	DFAILC = (F_1^{cu} / E_1) [DFAILC < 0]
DFAILM	Max strain for matrix straining in tension and compression	DFAILM ≥ max[(YT/EB) , (YC/EB)]
DFAILS	Max shear strain	0 < DFAILS ≤ 0.1
EFS	Effective failure strain	EFS = 0
TFAIL	Time step size criterion for element deletion	0 < TFAIL < (Δt/10)
ALPH	Shear stress nonlinear term	1E-3 ≤ ALPH ≤ 1
SOFT	Crush front strength-reducing parameter	Must be calibrated for crash simulations
FBRT	Softening factor for fiber tensile strength after matrix failure	0 ≤ FBRT ≤ 1
YCFAC	Softening factor for fiber compressive strength after matrix failure	0 ≤ YCFAC ≤ (XC/YC)
BETA	Weighting factor for shear term in tensile fiber mode	0 ≤ BETA ≤ 1
XC	Longitudinal compressive strength	$\lvert F_1^{cu} \rvert$, from material properties
XT	Longitudinal tensile strength	F_1^{tu}, from material properties
YC	Transverse compressive strength	$\lvert F_2^{cu} \rvert$, from material properties
YT	Transverse tensile strength	F_2^{tu}, from properties
SC	Shear strength	F_{12}^{tu}, from material properties
CRIT	Failure criterion used (MAT54 Chang-Chang, MAT55 Tsai-Wu)	Assign value of 54 or 55
*If using U.S. units, divide by a gravity factor to convert from pound-weight to pound-mass.		

APPENDIX C—BASELINE MAT54 INPUT CARDS FOR UNIDIRECTIONAL TAPE AND PLAIN-WEAVE FABRIC MATERIALS

The baseline MAT54 input cards for the Advanced General Aviation Transport Experiment (AGATE) unidirectional tape and the AGATE plain-weave materials are given in figures C-1 and C-2, respectively.

***MAT_054 (ENHANCED_COMPOSITE_DAMAGE)**							
mid	**ro**	**Ea**	**eb**	**ec**	**prba**	**prca**	**prcb**
1	1.50E-4	1.84E+7	1.22E+6	0.0	0.02049	0.0	0.0
gab	**gbc**	**Gca**	**kf**	**aopt**			
6.10E+5	6.10E+5	6.10E+5	0.0	0.0			
xp	**yp**	**Zp**	**a1**	**a2**	**a3**	**mangle**	
0.0	0.0	0.0	0.0	0.0	0.0	0.0	
v1	**v2**	**v3**	**d1**	**d2**	**d3**	**dfailm**	**dfails**
0.0	0.0	0.0	0.0	0.0	0.0	0.024	0.03
tfail	**alph**	**Soft**	**fbrt**	**ycfac**	**dfailt**	**dfailc**	**efs**
1.1530E-9	0.1	0.0	0.5	1.2	0.0174	-0.0116	0.0
xc	**xt**	**Yc**	**yt**	**sc**	**crit**	**beta**	
213000	319000	28800	7090	22400	54	0.5	

Figure C-1. Baseline MAT54 Material Card for the AGATE Unidirectional Tape Material

***MAT_054 (ENHANCED_COMPOSITE_DAMAGE)**							
mid	**ro**	**Ea**	**Eb**	**ec**	**prba**	**prca**	**prcb**
2	1.50E-4	8.11E+6	7.89E+6	0.0	0.043	0.0	0.0
gab	**gbc**	**Gca**	**Kf**	**aopt**			
6.09E+5	6.09E+5	6.09E+5	0.0	0.0			
xp	**yp**	**Zp**	**a1**	**a2**	**a3**	**mangle**	
0.0	0.0	0.0	0.0	0.0	0.0	0.000	
v1	**v2**	**v3**	**d1**	**d2**	**d3**	**dfailm**	**dfails**
0.0	0.0	0.0	0.0	0.0	0.0	0.014	0.03
tfail	**alph**	**Soft**	**Fbrt**	**ycfac**	**dfailt**	**dfailc**	**Efs**
1.1530E-9	0.1	0.0	0.5	1.2	0.0164	-0.013	0.0
xc	**xt**	**Yc**	**Yt**	**sc**	**crit**	**beta**	
103000	132000	102000	112000	19000	54	0.5	

Figure C-2. Baseline MAT54 Material Card for the AGATE Plain-Weave Fabric Material